SEISMIC EVALUTION OF REINFORCED CONCRETE FRAMED STRUCTURES

(A MAJOR PROJECT THESIS)

Submitted in the partial fulfilment of the requirements
for the award of the degree

MASTER OF TECHNOLOGY IN CIVIL ENGINEERING
With Specialization in
STRUCTURAL ENGINEERING

Submitted By
VINAY KUMAR SINGH
ROLL NO. 2K12/STE/023

Under the guidance of
PROF. A. K. GUPTA

DEPARTMENT OF CIVIL ENGINEERING
DELHI TECHNOLOGICAL UNIVERSITY
SHAHBAD DAULATPUR, BAWANA ROAD
DELHI-110042, INDIA

JULY 2014

DEPARTMENT OF CIVIL ENGINEERING

DELHI TECHNOLOGICAL UNIVERSITY

DELHI – 110042 (INDIA)

CANDIDATE'S DECLARATION

I do hereby certify that the work presented in the dissertation entitled "Seismic Evaluation of Reinforced Concrete Framed Structures" in the partial fulfilment of the requirements for the award of the degree of "Master of Technology" in Structural Engineering submitted in the Department of Civil Engineering, Delhi Technological University, is an authentic record of my own work carried out from August 2013 to July 2014 under the supervision of Prof. A. K. Gupta, Department of Civil Engineering.

I have not submitted the matter embodied in the dissertation for the award of other degree or diploma.

Date: 25th JULY 2014

Vinay Kumar Singh (2K12/STE/023)

This is to certify that above statement made by the candidate is correct to best of my knowledge.

Prof. A. K. Gupta

Department of Civil Engineering

Delhi Technological University

ACKNOWLEDGEMENT

I would like to express my sincere gratitude to my project guide Prof. A. K. Gupta for giving me the opportunity to work on this topic. It would never be possible for me to complete this project without his precious guidance and his relentless support and encouragement.

I would also like to present my sincere regards to my Head of Civil Engineering Department *Dr. A.K. Trivedi*, for his support and encouragement throughout the programme.

I am also thankful to all the faculty members and my classmates for the support and motivation during this work.

Last but not least, I specially thank all the people who are active in this field.

VINAY KUMAR SINGH

M. Tech. (Structure Engineering)

2K12/STE/023

ABSTRACT

In last decade, Bhuj earthquake of 2001 raised the questions about the adequacy of framed structures to resist strong seismic motions. Under such circumstances, to evaluate the performance of reinforced concrete (RC) framed buildings for future expected earthquakes, a non-linear static (pushover) analysis can be conducted. Pushover analysis evaluates the performance level of the building components and maximum base shear carrying capacity of the structure for various zones. This analysis is carried out for hinge properties, available in programs based on the FEMA-356 and ATC-40 guidelines.

Prediction of non-linear parameters of shear hinge in RC members is difficult because it involves a number of parameters like shear capacity, shear displacement, and shear stiffness. As shear failure is brittle in nature, designer must ensure that flexural failure (ductile mode of failure) precedes the shear failure. However, past earthquakes reveal that majority of the RC framed structures failed due to shear. Therefore, accurate modelling of shear failure is almost certain for seismic evaluation of RC framed building. The current industry practice is to do non-linear static (pushover) analysis for flexure only. To demonstrate the importance of modelling shear hinges a RC framed building, G+4 in zone-IV is selected. Two building models, one with shear hinge and other without shear hinges, are analysed using non-linear static (pushover) analysis. This study found that modelling shear hinges is necessary to correctly evaluate strength and ductility of the building. When analysis ignores shear failure model it overestimates the base shear and roof displacement capacity of the building. The results obtained here show that the presence of shear hinge can correctly reveal the non-ductile failure mode of the building. Therefore, the primary objective of the present work is to demonstrate the importance of modelling shear hinge in seismic evaluation of RC framed building.

LIST OF TABLES

LIST OF FIGURES

CONTENTS

CHAPTER 1.

INTRODUCTION

1.1 General

The earthquake of Bhuj, 2001 demonstrates that the most of buildings collapsed were found deficient to meet out the requirements of the present day codes It has raised the questions about the adequacy of framed structures to resist strong motions, since many buildings suffered great damage or collapsed. However, past earthquakes reveal that majority of the reinforced concrete (RC) structures failed due to shear. Indian construction practice does not guaranty safety against shear. A thorough literature review does not reveal any information about the nonlinear modelling of RC sections in Shear. The current industry practice is to do nonlinear analysis for flexure only. Designer has to design the sections such that flexural failure (ductile mode of failure) precedes the shear failure As shear failure are brittle in nature, designer must ensure that shear failure can never occur. Therefore, the primary objective of the present work is to develop nonlinear force-deformation model for reinforced concrete section for shear and demonstrate the importance of modelling shear hinge in seismic evaluation of RC framed building. From the existing literature it is found that equations given in Indian Standard IS-456: 2000 and American Standard ACI-318: 2008 represent good estimate of ultimate shear strength. However, FEMA-356 recommends ignoring concrete contribution in shear strength calculation for ductile beam under earthquake loading. No clarity is found regarding yield strength from the literature.

A pushover analysis is performed by subjecting a structure to a monotonically increasing pattern of lateral loads, representing the inertial forces which would be experienced by the structure when subjected to ground shaking. Under incrementally increasing loads various structural elements may yield sequentially. Consequently, at each event, the structure experiences a loss in stiffness. Using a pushover analysis, a characteristic nonlinear force-displacement relationship can be determined.

To demonstrate the importance of modelling shear hinges, an existing RC framed building is selected. Two building models, one with shear hinge and other without

shear hinges, are analysed using nonlinear static (pushover) analysis. Modelling shear hinges is necessary to correctly evaluate strength and ductility of the building. When analysis ignores shear failure model it overestimates the base shear and roof displacement capacity of the building. The results obtained here show that the presence of shear hinge can correctly reveal the non-ductile failure mode of the building.

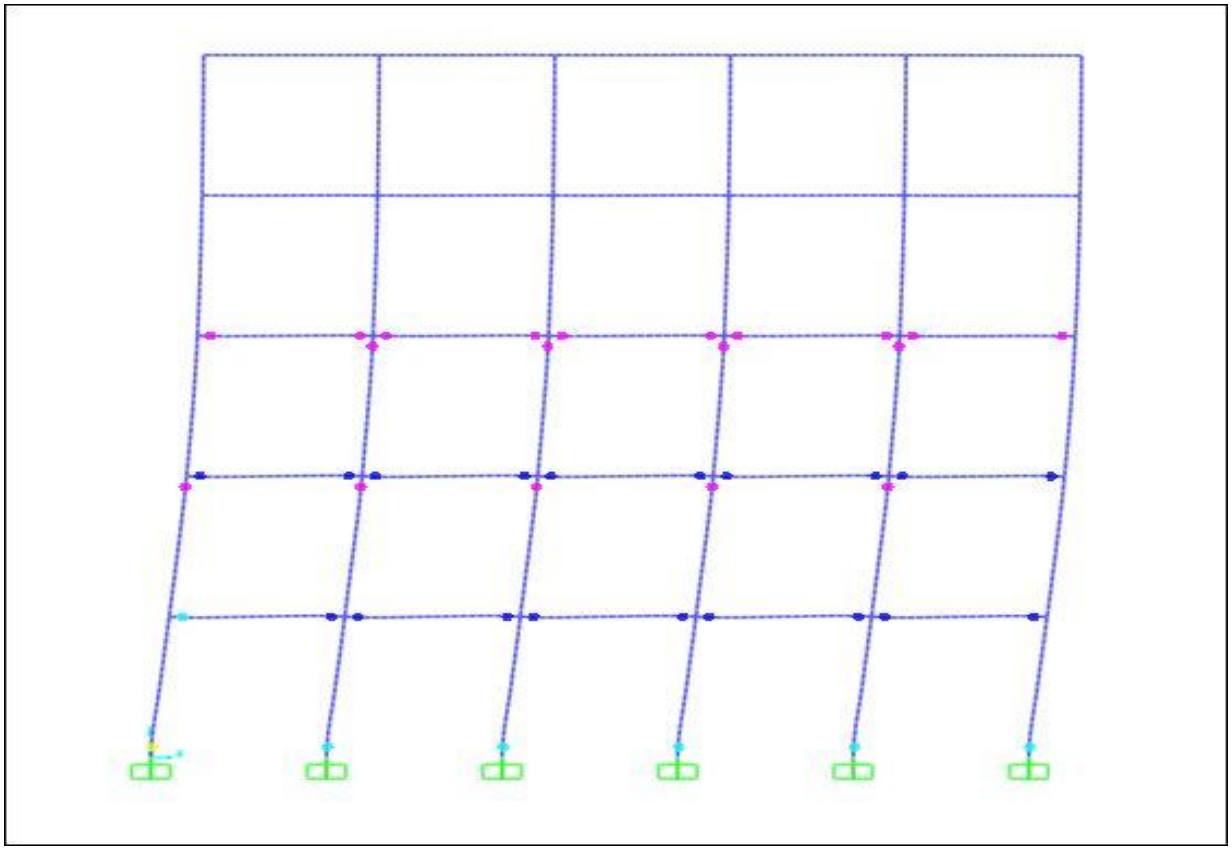

Fig: 1.1 Deformed shape of a building model under pushover loading

Fig: 1.1 represents deformed shape of a building model under nonlinear lateral load. Failure through formation of hinges in the columns is also shown in this figure. A nonlinear analysis can predict the failure mode, maximum force and deformation capacity of the structure. But to do an accurate analysis nonlinear modelling of frame sections for flexure and shear is very important.

Moment-rotation parameters are the actual input for modelling the hinge properties and this can be calculated from the moment-curvature relation. plastic hinges with limit capacities on deformation can be defined for all six degrees of freedom, namely,

axial force, transverse shear forces in X- and Y-directions, moments about Y- and Z-axes, and torsion (moment about X-axis).

A typical response at a plastic hinge can be considered as shown in Fig: 1.2. The main points in the moment-rotation curve shown in the Fig1.2 can be defined as follows:

• The point ‘A’ corresponds to the unloaded condition.

• The point ‘B’ corresponds to the nominal yield strength and yield rotation θy

• The point ‘C’ corresponds to the ultimate strength and ultimate rotation θu, following which failure takes place.

• The point ‘D’ corresponds to the residual strength, if any, in the member. It is usually limited to 20% of the yield strength, and ultimate rotation, θu can be taken with that.

• The point ‘E’ defines the maximum deformation capacity and is taken as 15θy or

θu, whichever is greater.

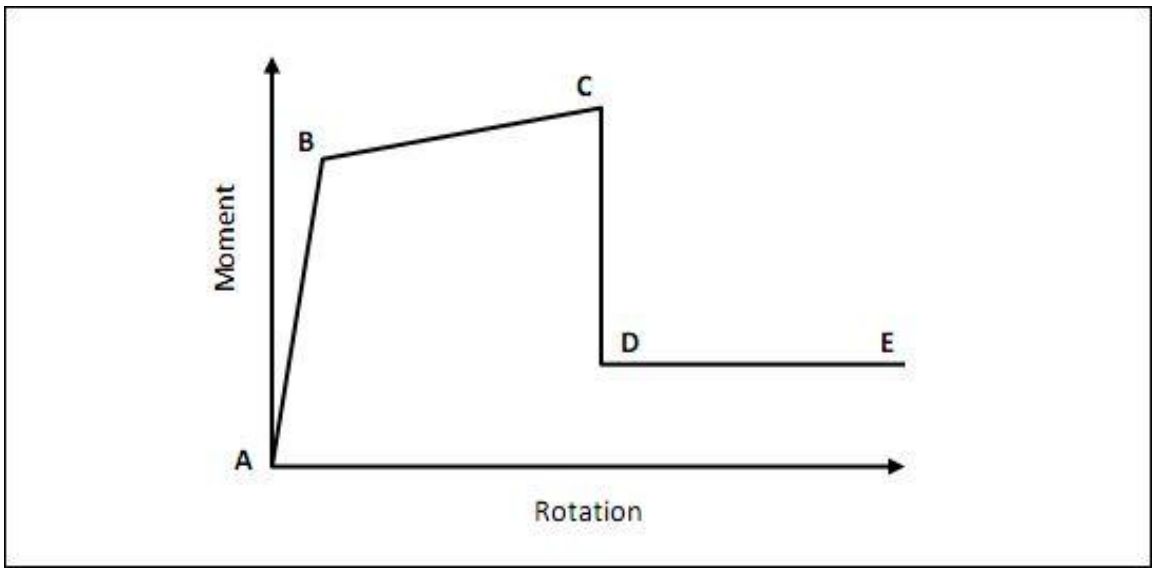

Fig: 1.2 Idealised Moment-rotation curve of RC elements

Fig. 1.2 presents a typical nonlinear moment rotation curve for RC member. Alternative methods are available in literature to calculate the important points required to define the nonlinear moment rotation curve for any section. In the conventional analysis the sections are generally considered to be elastic in shear although this is not true. It is important to check how nonlinear modelling of shear

alters the seismic behaviour of RC framed building. In the frame structure, the analyst identifies the possible locations for plastic hinge formation from his experience. Mathematically, nonlinear static analysis does not lead to a unique solution. Small changes in properties or sequence of loading can lead to large variations in the nonlinear response.

1.2 Objective

The objectives of this dissertation can be summarized as follows:

(i) To develop a detailed literature review on behaviour of shear in RC rectangular sections to determine nonlinear modelling parameters.

(ii) To develop nonlinear modelling parameters of rectangular RC members with transverse reinforcement in shear.

(iii) To carry out a seismic evaluation of a RC framed building considering nonlinearity in shear as well as flexure using the developed modelling parameters.

(iv) Two building models, one with shear hinge and other without shear hinges, are analysed using non-linear static (pushover) analysis.

1.3 Scope of the present study

a) Only rectangular sections are considered for the present study.
b) Spiral web reinforcement is kept outside the scope of the present study.
c) Stress-strain relation for reinforcing steel is taken from the IS 456:2000.
d) The nonlinear shear hinge properties of rectangular RC sections developed here can be validated through experimental study.

1.4 Methodology of the work

1. Detailed literature review on behaviour of shear in RC rectangular sections to determine nonlinear modelling parameters (shear capacity, shear displacement, yield and ultimate failure point).
2. Study of major international design codes with regard to the shear provisions are– Indian Standard IS 456: 2000, American Standard ACI 318: 2008 and FEMA 356: 2000.
3. Details of the selected RC framed building for the case study and computational modelling details of selected buildings.
4. Detail of the modelling of nonlinear force deformations behaviour for flexural and shear hinges.
5. Nonlinear pushover analysis (SAP2000) of the selected building is Analysed for two building models, one without shear hinges and other with shear hinges, and for two orthogonal lateral directions (X and Y) of each model.
6. Two resulting capacity curves for Push X and for Push Y analysis are plotted.
7. Demonstrating the importance of modelling of shear hinges to correctly evaluate strength and ductility of the building. Presence of shear hinge can correctly reveal the non-ductile failure mode of the building.
8. The results and conclusion.

CHAPTER 2.

LITERATURE REVIEW

2.1 Overview

Estimating seismic demands at low performance levels, such as life safety and collapse prevention, requires explicit consideration of inelastic behaviour of the structure. While nonlinear response history analysis is the most rigorous procedure to compute seismic demands, current civil engineering practice prefers to use the nonlinear static procedure (NSP) or pushover analysis. Although pushover analysis procedures have been proposed in several documents, the most commonly used pushover analysis is that specified in the FEMA-356 document (ASCE 2000). In early version of the FEMA NSP procedure (ATC 1997a, b), the seismic demands are computed by nonlinear static analysis of the structure subjected to monotonically increasing lateral forces with an invariant height-wise distribution until a predetermined target displacement is reached. Both the force distribution and target displacement are based on the assumption that the response is controlled by the fundamental mode and that the mode shape remains unchanged after the structure yields.

In past few years, several researchers have discussed the underlying assumptions and limitations of the pushover analysis (Elnashai 2001, Fajfar) and Gaspersic 1996, Gupta and Krawinkler 1999, Maison and Bonowitz 1999, Reinhorn 1997, Skokan and Hart 2000). It has been found that satisfactory predictions of seismic demands are mostly restricted to low-and medium-rise structures for which higher mode effects are likely to be minimal and the inelastic action is distributed throughout the height of the structure (Krawinkler and Seneviratna 1998).

The FEMA documents also recognized the inability of the NSP in accurately predicting seismic demands of buildings with significant higher mode effects (ATC 1997b). Therefore, application of the NSP alone is restricted to building without higher mode effects. The NSP can be used for buildings with significant higher mode effects provided it is supplemented by the Linear Dynamic Procedure.

It is now widely recognized that the concepts and guidelines embodied in FEMA-356 contain the essential ingredients of a performance-based seismic design (PBSD)

procedure. Though this document was developed for use in seismic rehabilitation of existing buildings, the key elements of the methodology are designed to accommodate the provisions of a future performance-based standard. FEMA-356 is essentially a deterministic approach to PBSD. FEMA-350 (2000), on the other hand, is a guideline for new steel construction and contains a probabilistic approach to performance assessment. ATC-40 (1996) shares many common elements with FEMA-356 but is limited in scope to reinforced concrete buildings. There are other on-going efforts to expand and enhance existing FEMA-356 guidelines (such as the ATC-58 effort) or to develop an entirely new methodology (such as the collaborative effort within the Pacific Earthquake Engineering Research [PEER] centre).

An extensive literature review is carried out on the three subjects:

(a) Estimation of shear strength of RC section,

(b) Estimation of shear deformation capacity of RC section and

(c) Pushover analysis of RC framed buildings.

A number of literatures are found on the estimation of shear strength for RC sections with and without web reinforcement. Majority of the previous works on shear strength estimations are based on experimental study. However, there is only one published literature found on the estimation of shear displacement capacity of RC section. There is no literature available that demonstrate the pushover analysis of framed building considering shear failure.

Following section presents a brief report of the literature review carried out on the above mentioned subjects as part of this project.

Xu et. al. (2005): presented shear capability of reinforced concrete beams without stirrups using a fracture mechanics approach. The new analytical formula is developed to shows the contributions of the reinforcement ratio (ρ), shear span to depth ratio (a/d), concrete quality to shear strength and the size effect in shear fracture. Finally from this new formula, shear bearing capability of reinforced concrete beam without stirrups evaluated and compared to that calculated by using Gastebled and May (1998) model, the ACI 318: 1989 Code and CEB-FIP Model Code (1990) respectively. It is further confirmed that fracture mechanics can be applied to know both the mode II fracture toughness KIIc and mode II fracture energy

GIIF of concrete materials capability of reinforced concrete beams without stirrups to the assessment of shear bearing important to perform more pure mode II fracture tests for various concrete materials and also provides knowledge to develop analytical formula for shear fracture problems in reinforced concrete members.

Karayannis et. al. (2005) performed experimental investigations on shear capacity of RC rectangular beam with continuous spiral transverse reinforcement under monotonic loading. Three specimens consist of beam with common stirrups, spiral transversal reinforcement and spiral transversal reinforcement with favourably inclined leg with shear span ratio 2.67 5 constructed. Based on experimental results and the behavioural curve of tested beams they found that the specimens with continuous spiral reinforcements demonstrated 15% and 17% respectively higher shear strength than the beam with closed stirrups. Beam with spiral reinforcements with favourably inclined legs exhibited enhanced performance and rather ductile response whereas other beam shows brittle shear failure.

Chowdhury (2007) developed a suitable hysteretic model that would predict the lateral deformation behaviour of lightly reinforced or shear-critical columns subjected to gravity and seismic load. Several tests on reinforced concrete columns under lateral loads have shown that the total drift stems from deformations owing to flexure, reinforcement slip, and shear. Existing analytical and experimental research on lightly reinforced columns is examined. This information is used for modify to ultimately develop a suitable overall hysteretic model that would accurately predict the lateral response of this class of columns with a limited computational effort. The behaviour of a column is classified into one of five categories based on a comparison of the shear, yield and flexural strengths. Overall the model did a reasonable job of simulating the load deformation relationships of shear-critical columns and provides a suitable platform to analyse older reinforced concrete buildings with a view to determining the amount of remediation necessary for satisfactory seismic performance.

Sezen and Setzler (2008) focused on modelling the behaviour of reinforced concrete columns subjected to lateral loads. Shear failure in columns initially dominated by flexural response is considered through the use of a shear capacity model. The proposed model was tested on 37 columns from various experimental studies. In general, the model predicted the lateral deformation response envelope reasonably

well. The focus of this research was the creation of a model that can predict the monotonic lateral force displacement relationship for reinforced 6 concrete columns subjected to lateral loading. The research concentrated on lightly reinforced columns that experience flexure-shear failures. However, the model can be applied to columns with any ratio of shear and flexural strengths. Therefore, it is applicable to columns that experience shear, flexure, or flexure-shear failures.

Kadid and Boumrkik (2008) evaluated the performance of framed buildings under earthquakes with the help of a nonlinear static pushover analysis. Three framed buildings were analyzed with 5, 8 and 12 stories respectively and results obtained from this study show that under seismic loads, properly designed frames will perform well. This study based on flexural hinge model concludes that the pushover analysis is relatively simple method to explore the nonlinear behaviour of buildings. By the intersection of the demand and capacity curves and the distribution of hinges in the beams and the columns, the behaviour of properly detailed 9 reinforced concrete frame building is adequately indicated. Most of the hinges are formed in the beams and few in the columns with limited damage.

Ahmad et. al. (2009) presented statistical model for the prediction of shear strength of high strength reinforced concrete (HSRC) beams. By comparing the actual and predicted values of shear strength of beams it shows that the proposed equation is conservatives for various longitudinal reinforcement ratios (ρ). It also compared the predicted values of shear strength to the values proposed by ACI, Russo et al. (2004), and Bazant et al. (1984). Bazant et al. (1984) is found to be un-conservative in estimating the shear stress for the HSRC beams without web reinforcement. The Russo et al. (2004) is more conservative as it underestimates the shear strength of the HSRC beams without web reinforcement. The ACI-318 equation for shear strength of HSRC beams gives some reasonable values when compared with the actual and predicted values. The Russo et al. (2004) on the other hand, is un-conservative for shear strength of HSRC beams with web reinforcement.

Paczkowski and Nowak (2008) reviewed the available data base and shear model for reinforced concrete beams without shear reinforcement and select the most efficient model for design code for concrete structure. The relationship between shear capacity and parameters such as width and depth of beam, longitudinal

reinforcement ratio and compressive strength of concrete has been established by using test results.

Zakaria et. al. (2009) present experimental investigations to clarify shear cracking behaviour of reinforced concrete beams. Test results show that shear reinforcement characteristics, longitudinal reinforcement ratios, the distance of shear crack from the crack tip and the intersections with nearest reinforcement's ratio play critical role in controlling diagonal crack spacing and openings. This research concluded that shear cracks width increases proportionally with both the strain of shear reinforcements and the spacing between the shear cracks. This implies that the stirrups strain and diagonal crack spacing are main factors on shear crack displacements.

Ghaffar et. al. (2010) verified the applications of shear strength equations available in literatures through experimental work. An extensive experimental study was carried out on rectangular reinforced concrete (RC) beams without web reinforcement. By considering three parameters, percentage of tension steel (P_t), compressive strength (f_{ck}) of concrete, and shear span to depth 4 ratio (a/d), new equations are developed for the shear strength estimation. Experimental results of the study show that the concrete shear capacity ranges from 1.7√fc´ to 1.8√fc´ before any cracking is observed. It shows that contribution of fc´ is about 80 to 90% of the total shear before any cracking which is against the Kani (1979). By considering divorcing point this study developed new equations for predictions of Cracking shear capacity and Ultimate shear capacity. Beam design may be economical if shear capacity supplied by new developed equations are kept in view.

Inel and Ozmen (2006) considered four and seven-story buildings to investigate the possible differences in the results of pushover analysis due to user defined nonlinear component properties for flexure. Pushover analysis is carried out assuming effective parameters like plastic hinge length and transverse reinforcement spacing for user-defined hinge properties. Plastic hinge length and transverse reinforcement spacing found to have no influence on the base shear capacity but they have considerable effects on the displacement capacity of the frames.

Displacement capacity improves by increasing the amount of transverse reinforcement. From this study they can observe that displacement capacity of the frames is greatly influenced by plastic hinge length (Lp). Comparisons show that

there is a variation of about 30% in displacement capacities due to plastic hinge length. Modern code compliant buildings may yield a reasonable capacity curve for the default-hinge model but this model is not suitable for other type of buildings. Also observations clearly show that in reflecting nonlinear behaviour compatible with the element properties the user-defined hinge model is better than the default-hinge model.

Rao and Injaganeri (2011) performed nonlinear analysis for developing the refined design models for both the cracking and ultimate shear strength of reinforced concrete beam without web reinforcement. The proposed models are functions of cylindrical compressive strength , longitudinal reinforcement ratio (ρ) and effective depth (d). The proposed models have been validated with the existing popular model as well as with the design code provisions. The study concluded that proposed model to predict the ultimate shear strength is simple and predicts shear strength of RC beams with fair degree of accuracy on the deep, short and normal beams.

Based on the literature review presented above salient objectives of the present study are defined as follows:

i) To develop nonlinear modelling parameters of rectangular RC members with transverse reinforcement in shear.

ii) To carry out a seismic evaluation case study of a RC framed building considering nonlinearity in shear as well as flexure using the developed modelling parameters.

Prediction of nonlinear shear hinge parameters in RC members is difficult because it involves a number of parameters like shear capacity, shear displacement, shear stiffness. Shear failure mostly occur in beams and columns owing to inadequate shear design. In non-linear analysis, this can be modelled by providing ‘shear hinges’. These hinges located at the same points as the flexural hinges near the beam column joints.

2.2 Nonlinear Static (Pushover) Analysis

Pushover analysis is a nonlinear static analysis for a reinforced concrete (RC) framed structure subjected to lateral loading. The gravity loads are applied, and then lateral loading is applied first in X-direction starting at the end of the gravity push, and next in Y-direction again starting at the end of the gravity push (Valles et al., 1996; CSI, 2000). The concept of plastic hinge is extremely important in the nonlinear analysis.

The pushover analysis may be carried out using force control or deformation control. In the first option, the structure is subjected to an incremental distribution of lateral force, and incremental displacements are calculated. In the second option, the structure is subjected to a deformation profile, and lateral forces needed to generate those displacements are computed. Since the deformation profile is unknown, the first option is commonly used. For the displacement control the user specifies the target maximum displacement at a control point. In certain software's, displacement control is not the same as applying displacement loading on the structure; displacement control is simply used to measure the displacement that results from the applied loads and to adjust the magnitude of the loading in an attempt to reach certain measured displacement value. The so-called displacement control in this case is essentially a modified form of the force control. The force control strategy can have following options: (i) uniform distribution, (ii) triangular distribution, (iii) generalised power distribution, and (iv) modal adaptive distribution with single or multiple mode participation.

Pushover analysis is defined as an analysis wherein a mathematical model directly incorporating the nonlinear load-deformation characteristics of individual components and elements of the building shall be subjected to monotonically increasing lateral loads representing inertia forces in an earthquake until a 'target displacement' is exceeded.

Target displacement is the maximum displacement (elastic plus inelastic) of the building at roof expected under selected earthquake ground motion. Pushover analysis assesses the structural performance by estimating the force and deformation capacity and seismic demand using a nonlinear static analysis algorithm. The seismic demand parameters are global displacements (at roof or any other reference point), storey drifts, storey forces, and component deformation and

component forces. Response characteristics that can be obtained from the pushover analysis are summarised as follows:

a) Estimates of force and displacement capacities of the structure. Sequence of the member yielding and the progress of the overall capacity curve.

b) Estimates of force (axial, shear and moment) demands on potentially brittle elements and deformation demands on ductile elements.

c) Estimates of global displacement demand, corresponding inter-storey drifts and damages on structural and non-structural elements expected under the earthquake ground motion considered.

d) Sequences of the failure of elements and the consequent effect on the overall structural stability.

e) Identification of the critical regions, where the inelastic deformations are expected to be high and identification of strength irregularities (in plan or in elevation) of the building.

2.2.1 Capacity and Demand curves

Capacity: The overall capacity of a structure depends on the strength and deformation capacities of the individual components of the structure. A Pushover analysis procedure uses a series of sequential elastic analysis, superimposed to approximate a force–displacement capacity diagram of the overall structure. The mathematical model of the structure is modified to account for reduced resistance of yielding components. A lateral force distribution is again applied until a predetermined limit is reached. Pushover capacity curves approximate how structure behaves after exceeding the elastic limits.

Demand: Ground motions during an earthquake produce complex horizontal displacement patterns in structure that may vary with time. Tracking this motion at every time step to determine structural design requirements is judged impractical. For nonlinear method it is easier and more direct to use a set of lateral displacement as a design condition for a given structure and ground motion, the displacement is an estimate of the maximum expected response of the building during ground motion. Typical seismic demand Vs. Capacity is shown in Fig

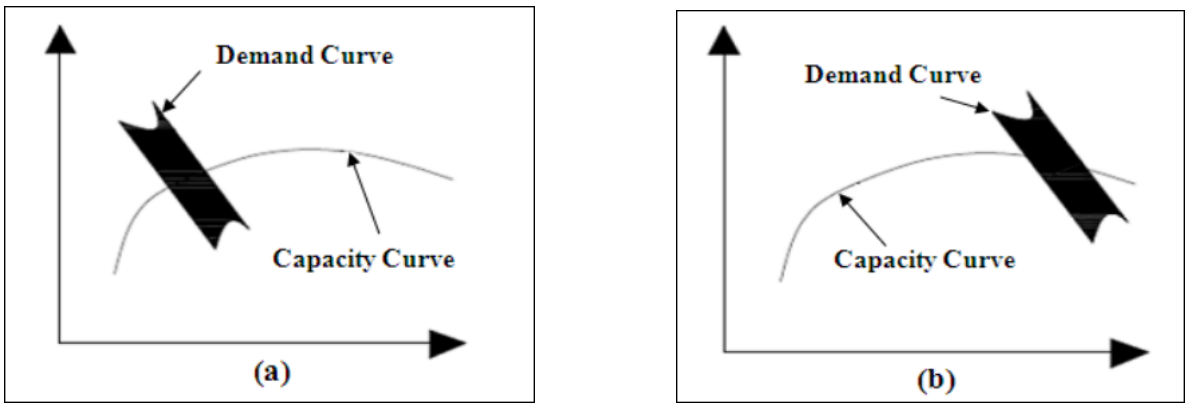

Fig: 2.1 Typical seismic demand Vs. Capacity (a) Safe Design (b) Unsafe Design

2.3 Shear Capacity

The shear capacity of a section is the maximum amount of shear the section can withstand before failure. Based on theoretical concept and experimental data researchers developed many equations to predict shear capacity but no unique solutions are available. Several equations are available to determine shear capacity of RC section, i.e., ACI 318:2005 equations, Zsutty's equation (1968,1971) and Kim and White equation (1991) etc. To verify the applicability of these equations experimental study was carried out by several researchers on rectangular RC beam with and without web reinforcement. Three parameters: cylindrical compressive strength, longitudinal reinforcement ratio (ρ) and shear span-to-depth ratio (a/d) are considered for developing equations for estimating shear strength of RC section without web reinforcement.

Factors affecting shear capacity of beam:

There are several parameters that affect the shear capacity of RC sections without web reinforcement. Following is a list of important parameters that can influence shear capacity of

RC section considerably:

1. Shear span to depth ratio (a/d)

2. Tension steel ratio (ρ)

3. Compressive strength of Concrete (fc)

4. Size of coarse aggregate

5. Density of concrete

6. Size of beam

7. Tensile strength of concrete

8. Support conditions

9. Clear span to depth ratio (L/d)

10. Number of layers of tension reinforcement

11. Grade of tension reinforcement

12. End anchorage of tension reinforcement.

The existing models available for shear capacity estimation for sections with and without web reinforcement. Shear capacity calculations for structural member are included as well. From this chapter it can be calculated that FEMA-356 does not consider contribution of concrete in shear strength calculation for beam under earthquake loading.

Contribution of web reinforcement in shear strength given in IS-456: 2000 and ACI-318: 2008 represent ultimate strength of the stirrups. FEMA-356 consider ultimate shear strength carried by the web reinforcement (= strength of the beam) as 1.05 times the yield strength hence no clarity in yield strength.

2.4 Shear Displacement

The shear forces are represented by V. The application of forces in such a manner causes the top of the element to slide with respect to the bottom. The effect of the shear forces translates into tension along the diagonal, which can be visualized by resolving the shear forces along the principal direction. As the concrete is weak in tension, it is susceptible to cracks in the direction perpendicular to the tensile load, which creates diagonal cracking well known to be associated with shear. The corresponding displacement is known as shear displacement (δ).

Deflections due to flexure and bond-slip are relatively easy to model with adequate accuracy whereas calculating shear displacement accurately has not been investigated thoroughly. The accuracy of the few existing models is not known. This chapter presents various methodologies available in literature to estimate shear displacement of RC section for un-cracked phase, at yield and at collapse.

Estimation of shear displacement capacity of RC section is an important part of the nonlinear shear failure modelling. There are very few published literatures available on this area.

2.5 Review of Code Provisions

This chapter reviews major international design codes with regard to the shear provision in RC section. This includes Indian Standard IS 456: 2000, American Standard ACI 318: 2008 and FEMA 356: 2000. The shear capacity of a section is the maximum amount of shear the beam can withstand before failure. In a RC member without shear reinforcement, shear force generally resisted by:

i) Shear resistance V_{cz} of the uncracked portion of concrete.

ii) Vertical component V_{ay} of the 'interface shear' (aggregate interlock) force V_a.

iii) Dowel force V_d in the tension reinforcement (due to dowel action).

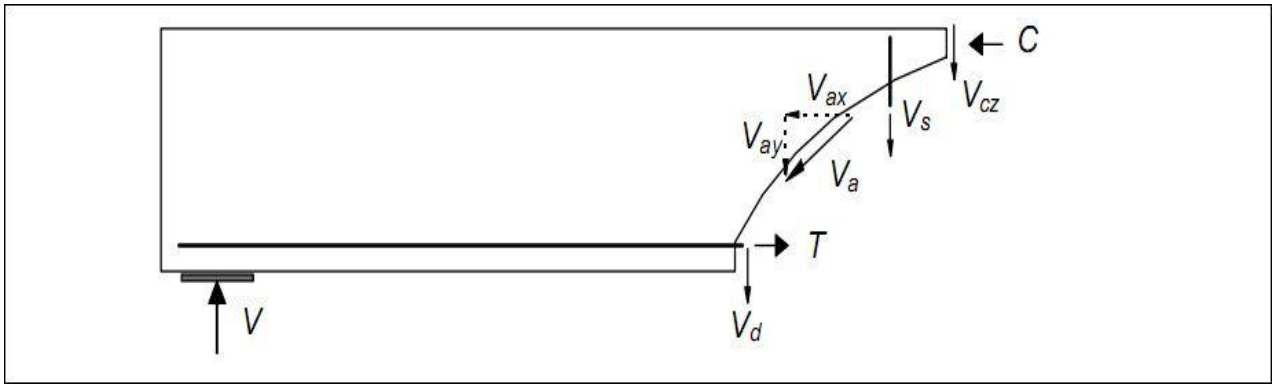

Fig: 2.2 Shear transfer mechanism

Member with shear reinforcement, shear force is mainly carried by uncracked portion of concrete (Vcz) and transverse reinforcement (Vs). Shear carried by aggregate interlock (Va) and dowel force in the tension reinforcement (Vd) are very small hence their effects are considered negligible.

International design codes except British Standard recommend procedures to calculate shear strength of rectangular and circular RC sections with transverse reinforcement. However, all the design codes are silent about the maximum shear displacement capacity of RC sections. Shear strength estimation procedures as per few major international codes are discussed as follows.

2.5.1 Indian Standard Code (IS 456: 2000):

Indian standard IS 456: 2000 as per Clause 40.1 specify the nominal shear stress by following equations.

$$\tau_v = \frac{V_u}{bd}$$

Shear carried by concrete is given by

$$V_u = \delta\, \tau_c\, bd$$

Where, $\delta = 1 + \frac{3P_u}{A_g f_{ck}} \leq 1.5$

And $\tau_c = \frac{0.85\sqrt{0.8f_{ck}}(\sqrt{1+5\beta}-1)}{6\beta}$

Here,$\beta = \frac{0.116 f_{ck}\, bd}{100\, A_{st}} \geq 1.0$

As per clause 40.2.2, for member subjected to axial compression P_u, the design shear strength of concrete, given in Table 19 shall be multiplied by the following factor: $\delta = 1 + \frac{3P_u}{A_g f_{ck}} \leq 1.5$

The design shear strength of concrete (τ_c) in beam without shear reinforcements is given in Table 19. τ_c Depend upon percentage of steel P_t which is given by

$$P_t = \frac{100A_{st}}{bd}$$

If τ_v exceeds τ_c given in Table 19, Shear reinforcement shall be provided in any of the following forms:

• Vertical stirrups

• Bent-up bars along with stirrups

• Inclined stirrups

Contribution of web reinforcement in shear strength given in IS-456: 2000 represent ultimate strength of the stirrups given by

$V_s = 0.87 f_y A_{sv} \frac{d}{S_v}$ For vertical stirrups

$V_s = 0.87 f_y A_{sv} \sin\alpha$ For bent up bars

$V_s = 0.87 f_y A_{sv} \frac{d}{S_v} (\sin\alpha + \cos\alpha)$ For inclined stirrups

2.5.2 American Concrete Institute (ACI318: 2008)

ACI 318: 2008, specify that the shear strength is based on an average shear stress on the full effective cross section $b_w d$. For a member without shear reinforcement, shear is assumed to be carried by the concrete web and member with shear reinforcement, a portion of the shear strength is assumed to be provided by the concrete and the remainder by the shear reinforcement.

As per clause 11.2,

$$V_y = V_c + V_s$$

$V_c = \delta \times (0.17\sqrt{f'_c})bd$ {Where, $\delta = 1 + \frac{Pu}{14A_g}$}

$V_s = \frac{A_{sv} \times f_{yh} \times d}{S_v}$ For vertical stirrups

$V_s = \frac{A_{sv} \times f_{yh} \times d}{S_v}(\sin\alpha + \cos\alpha)$ For inclined stirrups

2.5.3 Federal Emergency Management Agency (FEMA 356)

FEMA-356 does not consider contribution of concrete in shear strength calculation for beam under earthquake loading. FEMA-356 consider ultimate shear strength carried by the web reinforcement (= strength of the beam) as 1.05 times the yield strength. But there is no engineering background for this consideration.

CHAPTER 3.

STRUCTURAL MODELLING

3.1 Introduction

In the present study a RC framed building, G+4 are selected for seismic evaluation in zone-IV which is designed with IS 1893:2002 and IS 456:2000. This building is analysed considering nonlinear flexural and shear failure of the frame elements. All the analyses will be carried out in commercial software SAP 2000. Developing computational model is an important part on which linear or nonlinear, static or dynamic analysis performed. First part of this chapter explains the details of computational model. Also, details of the selected building model are described in this section. Accurate modelling of the nonlinear properties of various structural elements is very important in nonlinear analysis. Frame elements in this study are modelled with inelastic flexural hinges and shear hinges.

Concrete has been the most preferred construction material of the twentieth century, Over the last 50 years, the strengths of various types of concrete have increased from the low levels of 15-20 MPa to values in the range of 40-70 MPa. Strength-based designs are slowly giving way to performance-based designs where strength is only one of the criteria to be satisfied. There is an increased attention being paid to life prediction and maintenance scheduling. Finite element software is extensively used in design offices for the analysis and design of concrete structures. It may be worthwhile at this stage to exactly calibrate the status of present day analysis and design viz., the “realistic estimates” on load effects and deformations. Consider, for example, the design of a multi-storeyed framed structure. The load cases to be considered are the dead load, live load, wind load, seismic load, and their combinations. The input data that is normally fed into the computer software includes modulus of elasticity, Poisson’s ratio, density of concrete, areas and moments of inertia of all structural elements, basic wind speed, zoning factor for seismic loading, and so on. Then one goes on to define the load combinations to obtain the worst load effects.

Generally the gross section properties are used, and elastic analysis is performed. The design is based on the limit state philosophy. So the elastic load effects that are

obtained are multiplied by the load factors to obtain the capacity requirements. The design is based on the limit state design philosophy covering limit states of serviceability and collapse. The limit state of serviceability is deemed to be satisfied if all the recommendations given in IS: 456-2000 (BIS, 2000) regarding the detailing are satisfied.

.3.2 Computational Model

Modelling a building consist of the modelling and assemblage of its various load-carrying elements. A model must represent the 3D characteristics of building, including mass distribution, strength, stiffness and deformability. Modelling of the material properties and structural elements used in the present study is discussed below.

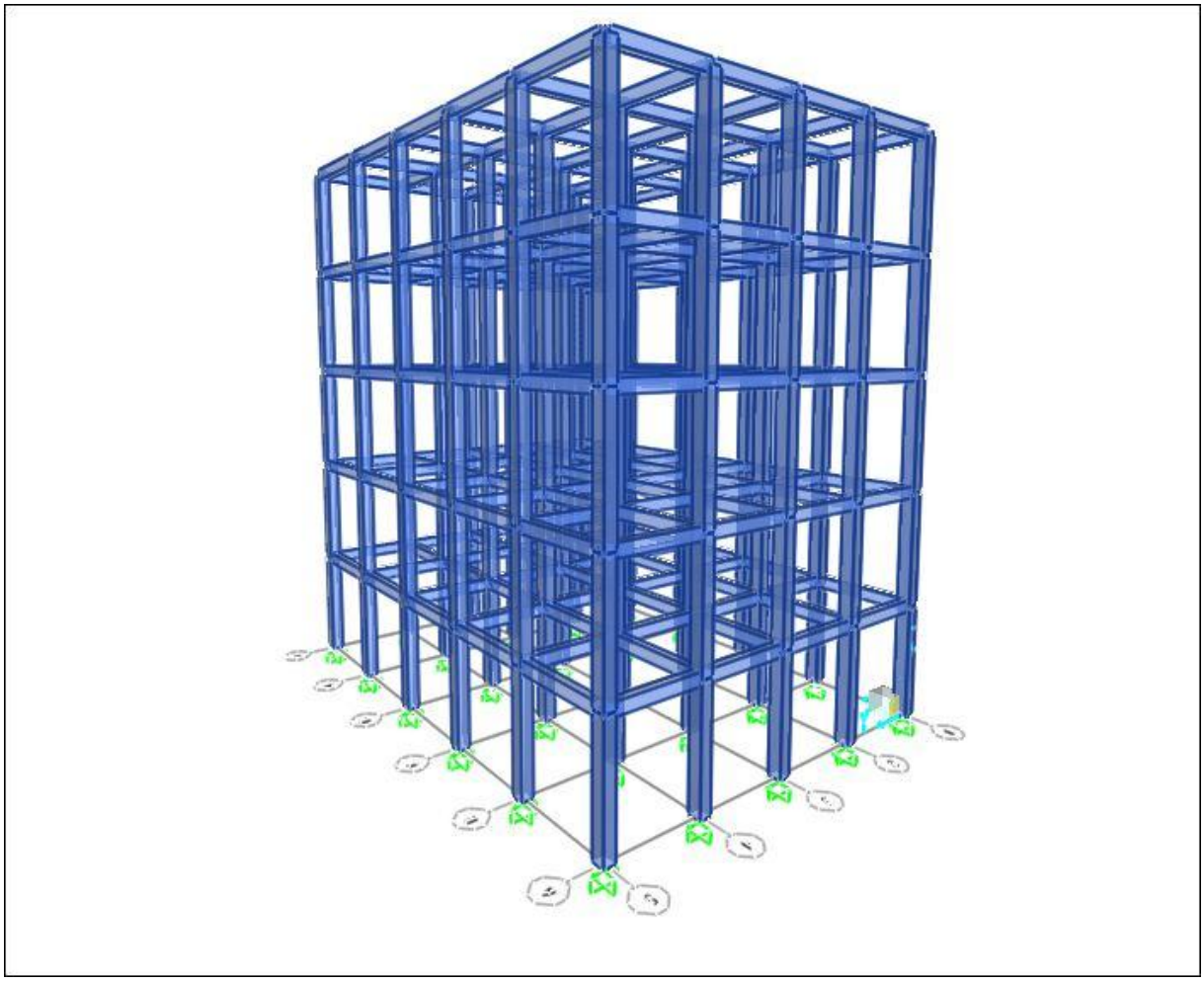

Fig: 3.1 Three dimensional view of the structure

3.2.1 Modelling of the Geometry

This section provides model geometry information, including items such as joint coordinates, joint restraints, and element connectivity.

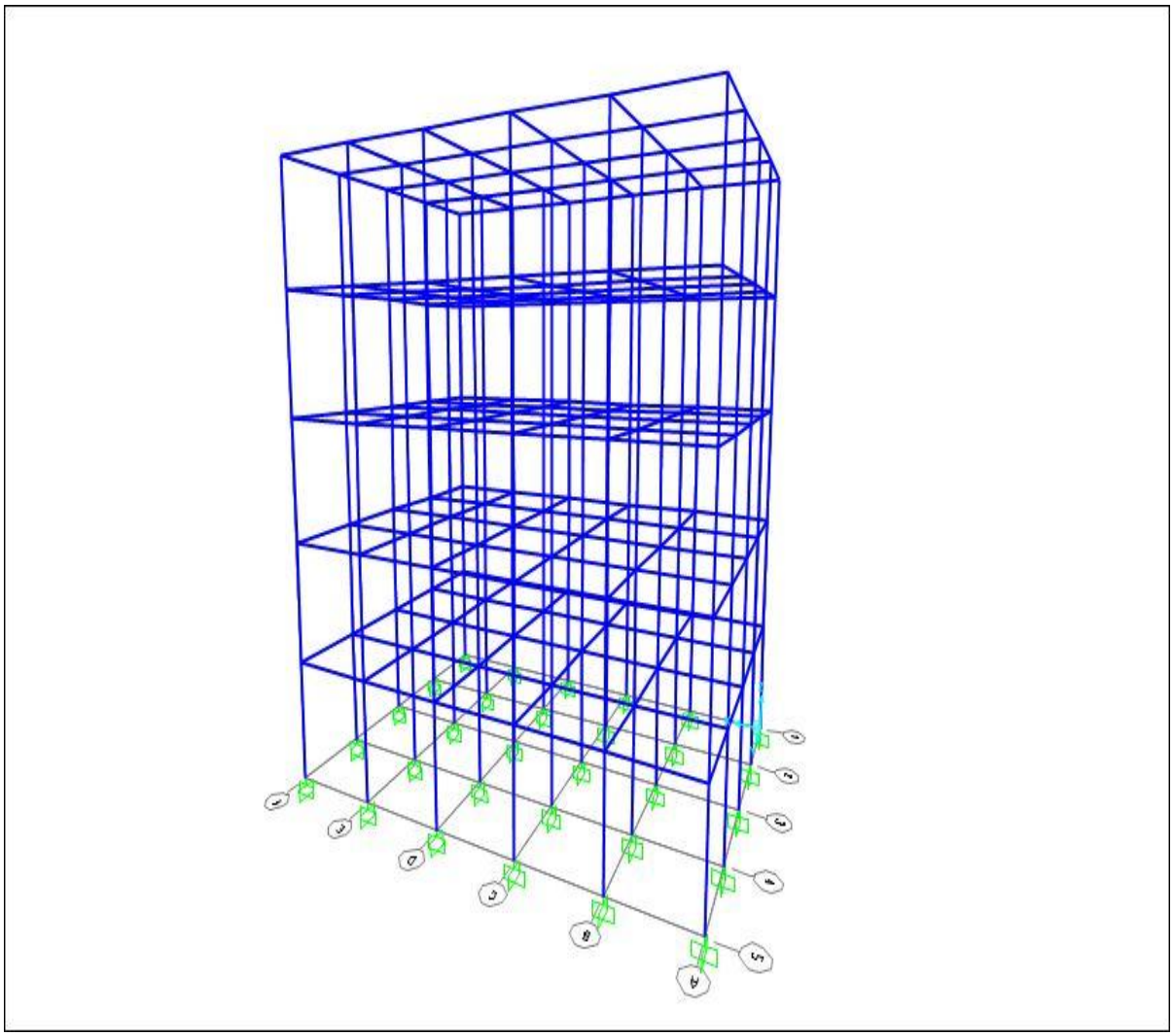

Fig: 3.2 Finite element model of the structure

Joint coordinates

Table 3.1: Joint Coordinates

Joint	Coord. Sys	Coord Type	Global X	Global Y	Global Z
			m	m	m
1	GLOBAL	Cartesian	0.00000	0.00000	0.00000
2	GLOBAL	Cartesian	0.00000	0.00000	3.50000
3	GLOBAL	Cartesian	0.00000	0.00000	7.00000
4	GLOBAL	Cartesian	0.00000	0.00000	10.50000
5	GLOBAL	Cartesian	0.00000	0.00000	14.00000
6	GLOBAL	Cartesian	0.00000	0.00000	17.50000
7	GLOBAL	Cartesian	0.00000	3.23000	0.00000
8	GLOBAL	Cartesian	0.00000	3.23000	3.50000
9	GLOBAL	Cartesian	0.00000	3.23000	7.00000
10	GLOBAL	Cartesian	0.00000	3.23000	10.50000
11	GLOBAL	Cartesian	0.00000	3.23000	14.00000
12	GLOBAL	Cartesian	0.00000	3.23000	17.50000
13	GLOBAL	Cartesian	0.00000	6.46000	0.00000
14	GLOBAL	Cartesian	0.00000	6.46000	3.50000
15	GLOBAL	Cartesian	0.00000	6.46000	7.00000
16	GLOBAL	Cartesian	0.00000	6.46000	10.50000
17	GLOBAL	Cartesian	0.00000	6.46000	14.00000
18	GLOBAL	Cartesian	0.00000	6.46000	17.50000
19	GLOBAL	Cartesian	0.00000	9.69000	0.00000
20	GLOBAL	Cartesian	0.00000	9.69000	3.50000
21	GLOBAL	Cartesian	0.00000	9.69000	7.00000
22	GLOBAL	Cartesian	0.00000	9.69000	10.50000
23	GLOBAL	Cartesian	0.00000	9.69000	14.00000
24	GLOBAL	Cartesian	0.00000	9.69000	17.50000
25	GLOBAL	Cartesian	0.00000	12.92000	0.00000
26	GLOBAL	Cartesian	0.00000	12.92000	3.50000
27	GLOBAL	Cartesian	0.00000	12.92000	7.00000
28	GLOBAL	Cartesian	0.00000	12.92000	10.50000
29	GLOBAL	Cartesian	0.00000	12.92000	14.00000
30	GLOBAL	Cartesian	0.00000	12.92000	17.50000
31	GLOBAL	Cartesian	3.23000	0.00000	0.00000

Table 3.1: Joint Coordinates

Joint	Coord. Sys	Coord Type	Global X	Global Y	Global Z
			m	m	m
32	GLOBAL	Cartesian	3.23000	0.00000	3.50000
33	GLOBAL	Cartesian	3.23000	0.00000	7.00000
34	GLOBAL	Cartesian	3.23000	0.00000	10.50000
35	GLOBAL	Cartesian	3.23000	0.00000	14.00000
36	GLOBAL	Cartesian	3.23000	0.00000	17.50000
37	GLOBAL	Cartesian	3.23000	3.23000	0.00000
38	GLOBAL	Cartesian	3.23000	3.23000	3.50000
39	GLOBAL	Cartesian	3.23000	3.23000	7.00000
40	GLOBAL	Cartesian	3.23000	3.23000	10.50000
41	GLOBAL	Cartesian	3.23000	3.23000	14.00000
42	GLOBAL	Cartesian	3.23000	3.23000	17.50000
43	GLOBAL	Cartesian	3.23000	6.46000	0.00000
44	GLOBAL	Cartesian	3.23000	6.46000	3.50000
45	GLOBAL	Cartesian	3.23000	6.46000	7.00000
46	GLOBAL	Cartesian	3.23000	6.46000	10.50000
47	GLOBAL	Cartesian	3.23000	6.46000	14.00000
48	GLOBAL	Cartesian	3.23000	6.46000	17.50000
49	GLOBAL	Cartesian	3.23000	9.69000	0.00000
50	GLOBAL	Cartesian	3.23000	9.69000	3.50000
51	GLOBAL	Cartesian	3.23000	9.69000	7.00000
52	GLOBAL	Cartesian	3.23000	9.69000	10.50000
53	GLOBAL	Cartesian	3.23000	9.69000	14.00000
54	GLOBAL	Cartesian	3.23000	9.69000	17.50000
55	GLOBAL	Cartesian	3.23000	12.92000	0.00000
56	GLOBAL	Cartesian	3.23000	12.92000	3.50000
57	GLOBAL	Cartesian	3.23000	12.92000	7.00000
58	GLOBAL	Cartesian	3.23000	12.92000	10.50000
59	GLOBAL	Cartesian	3.23000	12.92000	14.00000
60	GLOBAL	Cartesian	3.23000	12.92000	17.50000
61	GLOBAL	Cartesian	6.46000	0.00000	0.00000
62	GLOBAL	Cartesian	6.46000	0.00000	3.50000
63	GLOBAL	Cartesian	6.46000	0.00000	7.00000
64	GLOBAL	Cartesian	6.46000	0.00000	10.50000

Table 3.1: Joint Coordinates

Joint	Coord. Sys	Coord Type	Global X	Global Y	Global Z
			m	m	m
65	GLOBAL	Cartesian	6.46000	0.00000	14.00000
66	GLOBAL	Cartesian	6.46000	0.00000	17.50000
67	GLOBAL	Cartesian	6.46000	3.23000	0.00000
68	GLOBAL	Cartesian	6.46000	3.23000	3.50000
69	GLOBAL	Cartesian	6.46000	3.23000	7.00000
70	GLOBAL	Cartesian	6.46000	3.23000	10.50000
71	GLOBAL	Cartesian	6.46000	3.23000	14.00000
72	GLOBAL	Cartesian	6.46000	3.23000	17.50000
73	GLOBAL	Cartesian	6.46000	6.46000	0.00000
74	GLOBAL	Cartesian	6.46000	6.46000	3.50000
75	GLOBAL	Cartesian	6.46000	6.46000	7.00000
76	GLOBAL	Cartesian	6.46000	6.46000	10.50000
77	GLOBAL	Cartesian	6.46000	6.46000	14.00000
78	GLOBAL	Cartesian	6.46000	6.46000	17.50000
79	GLOBAL	Cartesian	6.46000	9.69000	0.00000
80	GLOBAL	Cartesian	6.46000	9.69000	3.50000
81	GLOBAL	Cartesian	6.46000	9.69000	7.00000
82	GLOBAL	Cartesian	6.46000	9.69000	10.50000
83	GLOBAL	Cartesian	6.46000	9.69000	14.00000
84	GLOBAL	Cartesian	6.46000	9.69000	17.50000
85	GLOBAL	Cartesian	6.46000	12.92000	0.00000
86	GLOBAL	Cartesian	6.46000	12.92000	3.50000
87	GLOBAL	Cartesian	6.46000	12.92000	7.00000
88	GLOBAL	Cartesian	6.46000	12.92000	10.50000
89	GLOBAL	Cartesian	6.46000	12.92000	14.00000
90	GLOBAL	Cartesian	6.46000	12.92000	17.50000
91	GLOBAL	Cartesian	9.69000	0.00000	0.00000
92	GLOBAL	Cartesian	9.69000	0.00000	3.50000
93	GLOBAL	Cartesian	9.69000	0.00000	7.00000
94	GLOBAL	Cartesian	9.69000	0.00000	10.50000
95	GLOBAL	Cartesian	9.69000	0.00000	14.00000
96	GLOBAL	Cartesian	9.69000	0.00000	17.50000
97	GLOBAL	Cartesian	9.69000	3.23000	0.00000

Table 3.1: Joint Coordinates

Joint	Coord. Sys	Coord Type	Global X	Global Y	Global Z
			m	m	m
98	GLOBAL	Cartesian	9.69000	3.23000	3.50000
99	GLOBAL	Cartesian	9.69000	3.23000	7.00000
100	GLOBAL	Cartesian	9.69000	3.23000	10.50000
101	GLOBAL	Cartesian	9.69000	3.23000	14.00000
102	GLOBAL	Cartesian	9.69000	3.23000	17.50000
103	GLOBAL	Cartesian	9.69000	6.46000	0.00000
104	GLOBAL	Cartesian	9.69000	6.46000	3.50000
105	GLOBAL	Cartesian	9.69000	6.46000	7.00000
106	GLOBAL	Cartesian	9.69000	6.46000	10.50000
107	GLOBAL	Cartesian	9.69000	6.46000	14.00000
108	GLOBAL	Cartesian	9.69000	6.46000	17.50000
109	GLOBAL	Cartesian	9.69000	9.69000	0.00000
110	GLOBAL	Cartesian	9.69000	9.69000	3.50000
111	GLOBAL	Cartesian	9.69000	9.69000	7.00000
112	GLOBAL	Cartesian	9.69000	9.69000	10.50000
113	GLOBAL	Cartesian	9.69000	9.69000	14.00000
114	GLOBAL	Cartesian	9.69000	9.69000	17.50000
115	GLOBAL	Cartesian	9.69000	12.92000	0.00000
116	GLOBAL	Cartesian	9.69000	12.92000	3.50000
117	GLOBAL	Cartesian	9.69000	12.92000	7.00000
118	GLOBAL	Cartesian	9.69000	12.92000	10.50000
119	GLOBAL	Cartesian	9.69000	12.92000	14.00000
120	GLOBAL	Cartesian	9.69000	12.92000	17.50000
121	GLOBAL	Cartesian	12.92000	0.00000	0.00000
122	GLOBAL	Cartesian	12.92000	0.00000	3.50000
123	GLOBAL	Cartesian	12.92000	0.00000	7.00000
124	GLOBAL	Cartesian	12.92000	0.00000	10.50000
125	GLOBAL	Cartesian	12.92000	0.00000	14.00000
126	GLOBAL	Cartesian	12.92000	0.00000	17.50000
127	GLOBAL	Cartesian	12.92000	3.23000	0.00000
128	GLOBAL	Cartesian	12.92000	3.23000	3.50000
129	GLOBAL	Cartesian	12.92000	3.23000	7.00000
130	GLOBAL	Cartesian	12.92000	3.23000	10.50000

Table 3.1: Joint Coordinates

Joint	Coord. Sys	Coord Type	Global X	Global Y	Global Z
			m	m	m
131	GLOBAL	Cartesian	12.92000	3.23000	14.00000
132	GLOBAL	Cartesian	12.92000	3.23000	17.50000
133	GLOBAL	Cartesian	12.92000	6.46000	0.00000
134	GLOBAL	Cartesian	12.92000	6.46000	3.50000
135	GLOBAL	Cartesian	12.92000	6.46000	7.00000
136	GLOBAL	Cartesian	12.92000	6.46000	10.50000
137	GLOBAL	Cartesian	12.92000	6.46000	14.00000
138	GLOBAL	Cartesian	12.92000	6.46000	17.50000
139	GLOBAL	Cartesian	12.92000	9.69000	0.00000
140	GLOBAL	Cartesian	12.92000	9.69000	3.50000
141	GLOBAL	Cartesian	12.92000	9.69000	7.00000
142	GLOBAL	Cartesian	12.92000	9.69000	10.50000
143	GLOBAL	Cartesian	12.92000	9.69000	14.00000
144	GLOBAL	Cartesian	12.92000	9.69000	17.50000
145	GLOBAL	Cartesian	12.92000	12.92000	0.00000
146	GLOBAL	Cartesian	12.92000	12.92000	3.50000
147	GLOBAL	Cartesian	12.92000	12.92000	7.00000
148	GLOBAL	Cartesian	12.92000	12.92000	10.50000
149	GLOBAL	Cartesian	12.92000	12.92000	14.00000
150	GLOBAL	Cartesian	12.92000	12.92000	17.50000

Joint restraints Assignments

Table 3.2: Joint Restraint Assignments

Joint	U1	U2	U3	R1	R2	R3
1	Yes	Yes	Yes	Yes	Yes	Yes
7	Yes	Yes	Yes	Yes	Yes	Yes
13	Yes	Yes	Yes	Yes	Yes	Yes
19	Yes	Yes	Yes	Yes	Yes	Yes
25	Yes	Yes	Yes	Yes	Yes	Yes
31	Yes	Yes	Yes	Yes	Yes	Yes
37	Yes	Yes	Yes	Yes	Yes	Yes
43	Yes	Yes	Yes	Yes	Yes	Yes
49	Yes	Yes	Yes	Yes	Yes	Yes
55	Yes	Yes	Yes	Yes	Yes	Yes
61	Yes	Yes	Yes	Yes	Yes	Yes
67	Yes	Yes	Yes	Yes	Yes	Yes
73	Yes	Yes	Yes	Yes	Yes	Yes
79	Yes	Yes	Yes	Yes	Yes	Yes
85	Yes	Yes	Yes	Yes	Yes	Yes
91	Yes	Yes	Yes	Yes	Yes	Yes
97	Yes	Yes	Yes	Yes	Yes	Yes
103	Yes	Yes	Yes	Yes	Yes	Yes
109	Yes	Yes	Yes	Yes	Yes	Yes
115	Yes	Yes	Yes	Yes	Yes	Yes
121	Yes	Yes	Yes	Yes	Yes	Yes
127	Yes	Yes	Yes	Yes	Yes	Yes
133	Yes	Yes	Yes	Yes	Yes	Yes
139	Yes	Yes	Yes	Yes	Yes	Yes
145	Yes	Yes	Yes	Yes	Yes	Yes

3.2.2 Material properties

This section provides material property information for materials used in the model.

Material Properties - Basic Mechanical Properties:

Table 3.3 : Material Properties - Basic Mechanical Properties

Material	Unit Weight	Unit Mass	E1	G12	U12	A1
	KN/m3	KN-s2/m4	KN/m2	KN/m2		1/C
HYSD 415	7.6973E+01	7.8490E+00	200000000.0			1.1700E-05
M 25	2.4993E+01	2.5485E+00	25000000.00	10416666.67	0.200000	9.9000E-06
Mild 250	7.6973E+01	7.8490E+00	200000000.0			1.1700E-05

Material Properties - Concrete Data

Table 3.4: Material Properties - Concrete Data

Material	Fc	Final Slope
	KN/m2	
M25	25000.00	-0.100000

Material Properties - Rebar Data

Table 3.5: Material Properties - Rebar Data

Material	Fy	Fu	Final Slope
	KN/m2	KN/m2	
HYSD415	415000.00	485000.00	-0.100000
Mild250	250000.00	410000.00	-0.100000

3.2.3 Section properties

This section provides section property information for objects used in the model.

Frame Section Properties 01 - General, Part 1 of 4

Table 3.6.1: Frame Section Properties 01 - General, Part 1 of 4

Section Name	Material	Shape	t3	t2	Area	Tors Const.	I33	I22
			m	m	m2	m4	m4	m4
BM	M25	Rectangular	0.35000	0.25000	0.08750	0.001020	0.000893	0.000456
COL	M25	Rectangular	0.35000	0.30000	0.10500	0.001526	0.001072	0.000788

Frame Section Properties 01 - General, Part 2 of 4

Table 3.6.2: Frame Section Properties 01 - General, Part 2 of 4

Section Name	AS2	AS3
	m2	m2
BM	0.07297	0.072917
COL	0.08750	0.087500

Frame Section Properties 01 - General, Part 3 of 4

Table-3.6.3 Frame Section Properties 01 - General, Part 3 of 4

Section Name	S33	S22	Z33	Z22	R33	R22
	m3	m3	m3	m3	m	m
BM	0.005104	0.003646	0.007656	0.005469	0.101036	0.072169
COL	0.006125	0.005250	0.009188	0.007875	0.101036	0.086603

Frame Section Properties 01 - General, Part 4 of 4

Table-3.6.4 Frame Section Properties 01 - General, Part 4 of 4

Section Name	A Mod	A2Mod	A3Mod	J Mod	I2Mod	I3Mod	M Mod	W Mod
BM	1.00000	1.00000	1.00000	1.00000	1.00000	1.00000	1.00000	1.00000
COL	1.00000	1.00000	1.00000	1.00000	1.00000	1.00000	1.00000	1.00000

Frame Section Properties 02 - Concrete Column, Part 1 of 2

Table-3.7.1 Frame Section Properties 02 - Concrete Column, Part 1 of 2

Section Name	Rebar Mat L	Rebar Mat C	Reinf. Config.	Lat Reinf	Cover	NumBars 3Dir	NumBars 2Dir
					m		
COL	HYSD415	Mild250	Rectangular	Ties	0.040000	3	3

Frame Section Properties 02 - Concrete Column, Part 2 of 2

Table-3.7.2 Frame Section Properties 02 - Concrete Column, Part 2 of2

Section Name	Bar Size L	Bar Size C	Spacing C	NumCBars2	NumCBars3
			m		
COL	20d	12d	0.15000	3	3

Frame Section Properties 03 - Concrete Beam, Part 1 of 2

Table-3.8.1 Frame Section Properties 03 - Concrete Beam, Part 1 of 2

Section Name	Rebar Mat L	Rebar Mat C	Top Cover	Bot Cover
			m	m
BM	HYSD415	Mild250	0.060000	0.060000

Frame Section Properties 03 - Concrete Beam, Part 2 of 2

Table-3.8.2 Frame Section Properties 03 - Concrete Beam, Part 2 of 2

Section Name	Top Left Area	Top Right Area	Bot Left Area	Bot Right Area
	m2	m2	m2	m2
BM	0.030000	0.030000	0.030000	0.030000

3.2.4 Load patterns

This section provides loading information as applied to the model.

Load Pattern Definitions

Table-3.9 Load Pattern Definitions

Load Pat	Design Type	Self-Wt. Mult.
DEAD	DEAD	1.000000
LIVE	LIVE	0.250000

Load Case Definitions

Table-3.10 Load Case Definitions

Case	Type	Initial Cond	Modal Case	Des Act Opt	Design Act
DEAD	Non Static	Zero		Prog Det	Non-Composite
MODAL	Lin Modal	Zero		Prog Det	Other
LIVE	Lin Static	Zero		Prog Det	Short-Term Composite
RSP	Lin Resp Spec		MODAL	Prog Det	Short-Term Composite
PUSH Y	Non Static	DEAD		Prog Det	Short-Term Composite

Static case load assignments

Table-3.11 Case - Static 1 - Load Assignments

Case	Load Type	Load Name	Load SF	Trans Acc SF m/sec2
DEAD	Load pattern	DEAD	1.000000	
LIVE	Load pattern	LIVE	0.250000	
PUSH Y	Accel	Accel UY		-1.00000

Response spectrum case load assignments

Case - Response Spectrum 1 – General

Table-3.12 Case - Response Spectrum 1 - General

Case	Modal Combo	GMCf1	GMCf2	Per Rigid	Dir. Combo	Damping Type	Const. Damp
		Cyc/sec	Cyc/sec				
RSP	CQC	1.0000E+00	0.0000E+00	SRSS	SRSS	Constant	0.0500

Case - Response Spectrum 2 - Load Assignments

Table-3.13 Case - Response Spectrum 2 - Load Assignments

Case	Load Type	Load Name	Coord. Sys	Function	Angle	Trans Acc SF
					Degrees	m/sec2
RSP	Acceleration	U1	GLOBAL	UNIFRS	0.000	1.00000

Function - Response Spectrum – User

Table-3.14 Function - Response Spectrum - User

Name	Period	Accel	Func. Damp
	Sec		
UNIFRS	0.000000	1.000000	0.050000
UNIFRS	1.000000	1.000000	

3.3 Structural Elements

Beams and columns are modelled by 3D frame elements. To obtain the bending moments and forces at the beam and column faces beam-column joints are modelled by giving end-offsets to the frame elements. The beam-column joints are as considered to be rigid .The column end at foundation assumed as fixed for all the models in this study. Nonlinear properties at the possible yield locations are to be considered for all the frame elements.

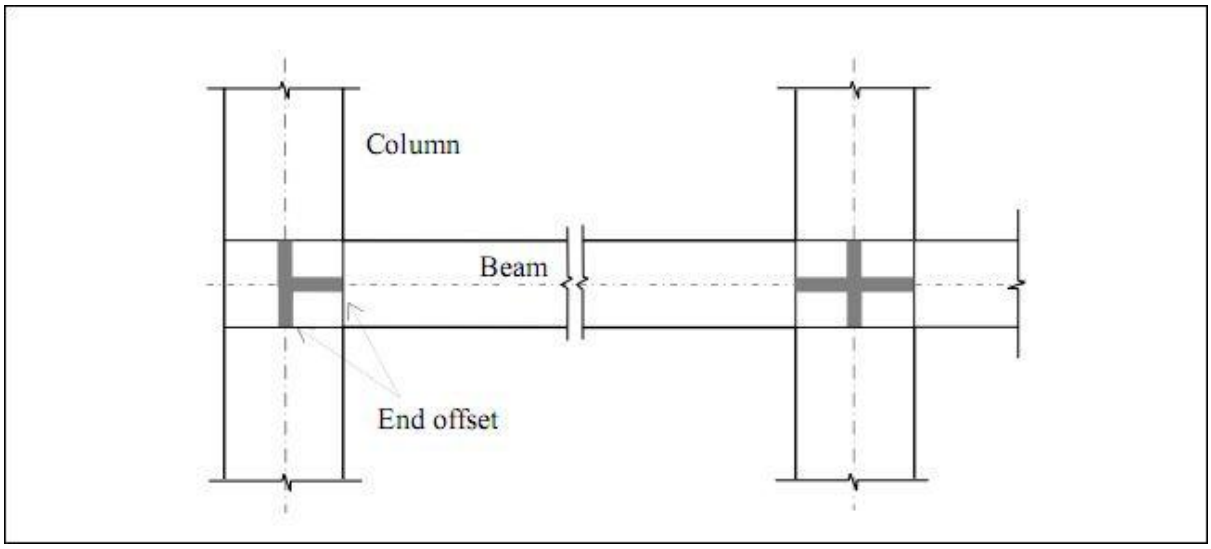

Fig: 3.3 Use of end offsets at beam-column joint

3.4 Modelling of Flexural Hinges

In the implementation of pushover analysis, the model must account for the nonlinear behaviour of the structural elements. In the present study, a point-plasticity approach is considered for modelling nonlinearity, wherein the plastic hinge is assumed to be concentrated at a specific point in the frame member under consideration. Beam and column elements in this study were modelled with flexure hinges at possible plastic regions under lateral load (i.e., both ends of the beams and columns).Properties of flexure hinges must simulate the actual response of reinforced concrete components subjected to lateral load. In the present study the plastic hinge properties are calculated by SAP 2000. The analytical procedure used to model the flexural plastic hinges are explained below.

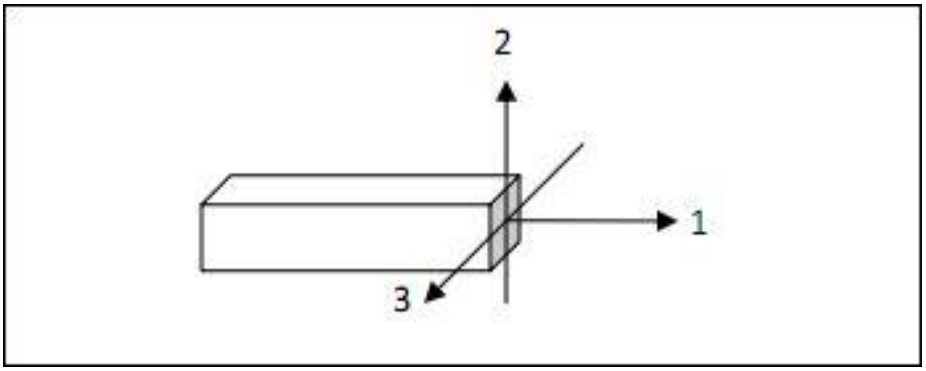

Fig: 3.4 The coordinate system used to define the flexural and shear hinges

Flexural hinges in this study are defined by moment-rotation curves calculated based on the cross-section and reinforcement details at the possible hinge locations. For calculating hinge properties it is required to carry out moment–curvature analysis of each element. Constitutive relations for concrete and reinforcing steel, plastic hinge length in structural element are required for this purpose. The flexural hinges in beams are modelled with uncoupled moment (M3) hinges whereas for column elements the flexural hinges are modelled with coupled P-M2-M3 properties that include the interaction of axial force and bi-axial bending moments at the hinge location. Although the axial force interaction is considered for column flexural hinges the rotation values were considered only for axial force associated with gravity load.

3.8 Modelling of Shear Hinges

When there is no prior failure in shear, flexural plastic hinges will develop along with the predicted values of ultimate moment capacity. Design codes prescribe specifications (e.g. ductile detailing requirement of IS 13920: 1993) for adequate shear reinforcement, corresponding to the ultimate moment capacity level. Therefore, it is obvious for a code designed building to fail in flexure and not in shear. There are a lot of buildings existing those are not detailed with IS 13920: 1993. Also, poor construction practise may lead to shear failure in framed building in the event of severe earthquakes.

Shear failure mostly occur in beams and columns owing to inadequate shear design. In non-linear analysis, this can be modelled by providing ‘shear hinges’. These hinges located at the same points as the flexural hinges near the beam column joints. If the shear hinge mechanism occurred before the formation of flexural hinge, the moment demand gets automatically restricted because of this flexural hinge may not develop.

In this section, procedure for generating shear force-deformation curves to assign shear hinges for beams and columns explained. It is assumed that shear force-deformation curves is symmetric for positive and negative shear forces.

Shear hinges for beams are modelled in one vertical direction (V2) whereas for columns shear hinges are modelled in two orthogonal horizontal directions (V2 and V3).

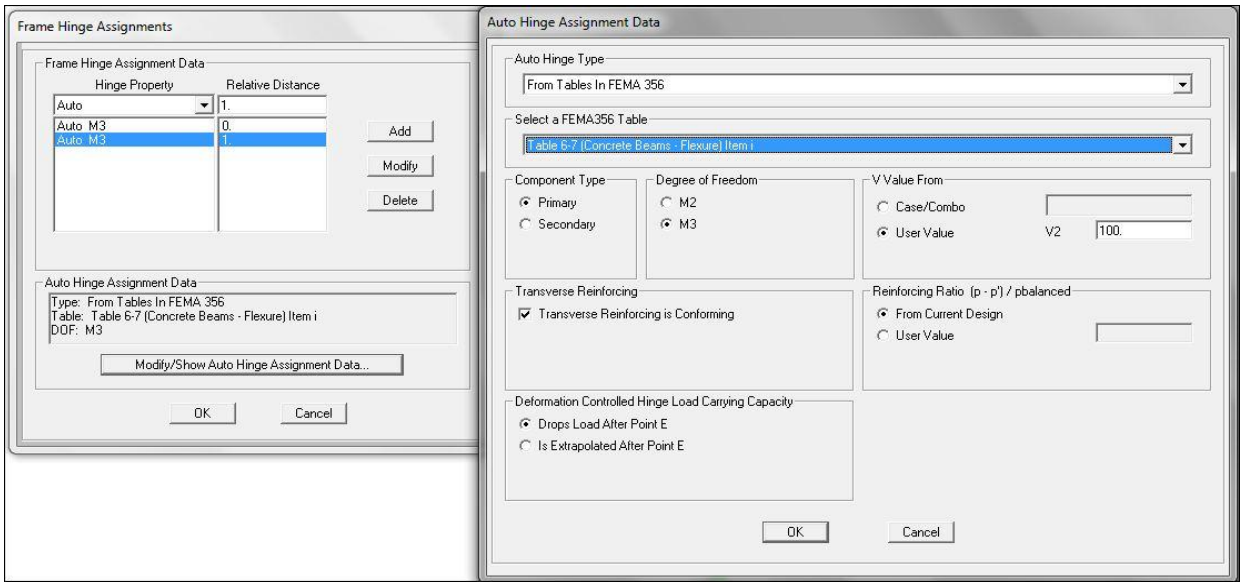

Fig: 3.5 Assigning shear hinge properties to the beam members

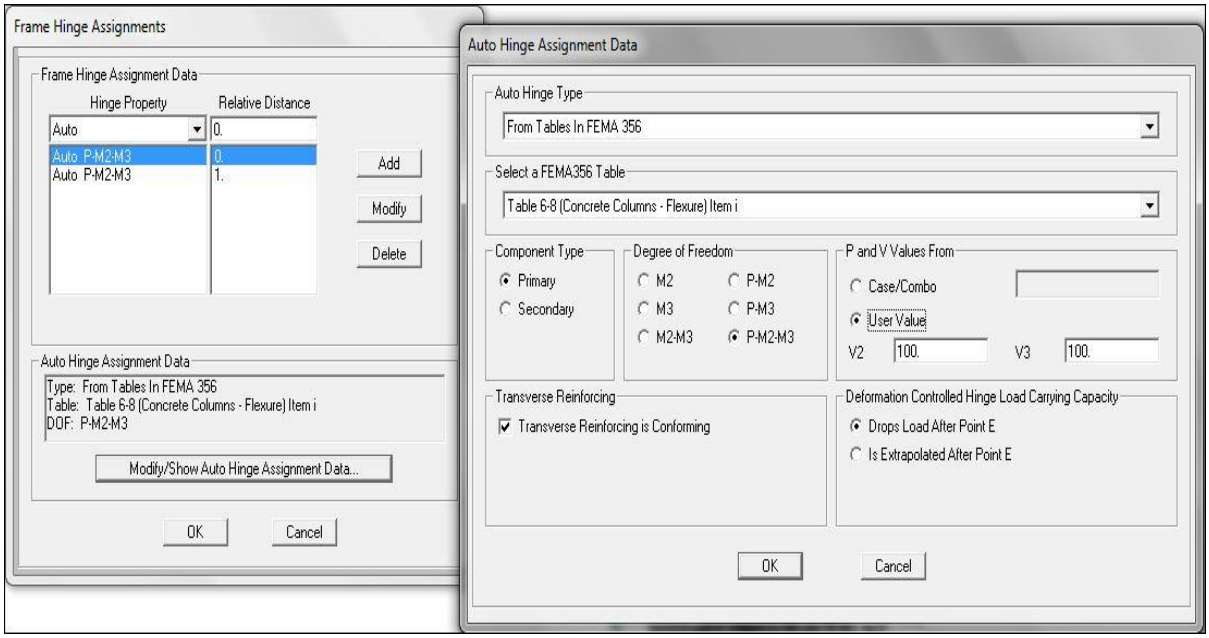

Fig: 3.6 Assigning shear hinge properties to the column members

CHAPTER 4.

NONLINEAR STATIC (PUSHOVER) ANALYSIS

4.1 Introduction

A nonlinear pushover analysis of the selected building is carried out as per FEMA 356 for evaluating the structural seismic response. In this analysis gravity loads and a representative lateral load pattern are applied to frame structure. The lateral loads were applied monotonically in a step-by-step manner. The applied lateral loads in X-direction representing the forces that would be experienced by the structures when subjected to ground shaking. The applied lateral forces were the product of mass and the first mode shape amplitude at each story level under consideration. P–Delta effects were also considered in account. At each stage, structural elements experience a stiffness change as shown in, where IO, LS and CP stand for immediate occupancy, life safety and collapse prevention respectively.

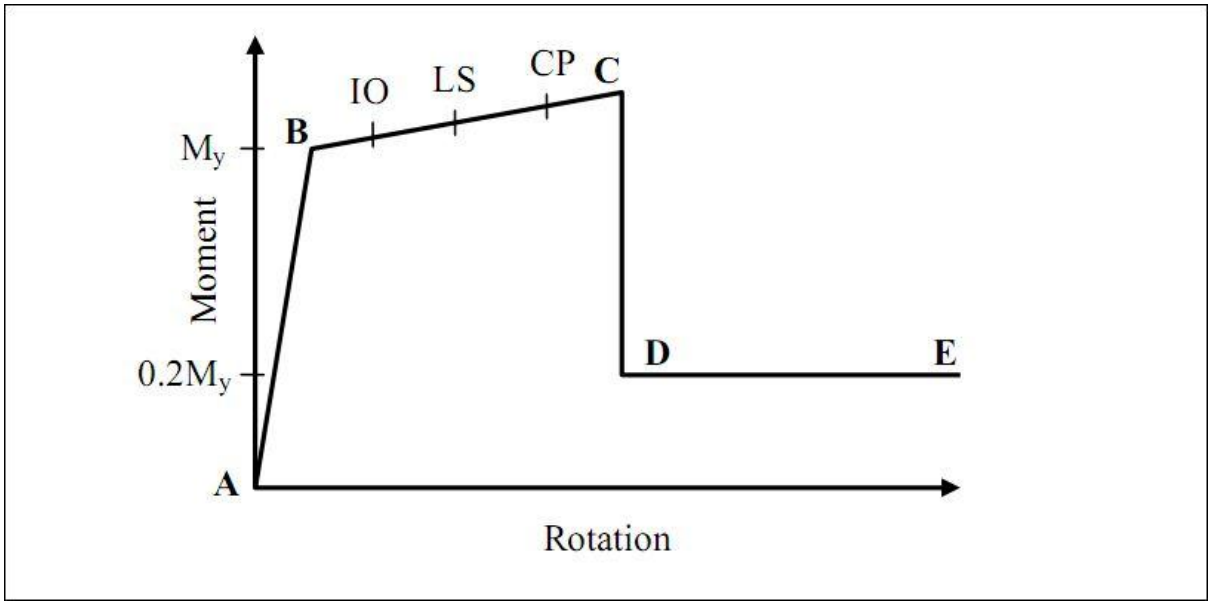

Fig: 4.1 Different stages of plastic hinge

It is a plot drawn between base shear and roof displacement. Performance point and location of hinges in various stages can be obtained from pushover curve as shown in Fig: 4.1 The range AB is elastic range, B to IO is the range of immediate occupancy IO to LS is the range of life safety and LS to CP is the range of collapse prevention. The Different Building performance levels are shown in table

Table-4.1 Different Building performance levels

Building Performance Levels				
	Collapse Prevention (CP) Level	Life Safety (LS) Level	Immediate Occupancy (IO) Level	Operational Level
Overall Damage	Severe	Moderate	light	Very light
General	Little residual stiffness and strength, but load bearing Columns and walls function. Large permanent drifts. Some exits blocked. In fills and unbraced Parapets failed or At incipient failure. Building is near collapse.	Some residual Strength and stiffness left in all stories. Gravity-load-bearing elements function. No Out-of-plane failure of walls or tipping of parapets. Some permanent drift. Damage to partitions. Building may be beyond economical repair.	No permanent drift. Structure substantially Retains original Strength and stiffness. Minor cracking of facades, partitions, and ceilings as well as structural elements. Elevators can be restarted. Fire protection operable.	No permanent drift; structure substantially Retains original strength and stiffness. Minor cracking of facades, partitions, and ceilings as well as structural elements. All Systems important to normal operation are functional.
Non-structural Components	Extensive damage.	Falling hazards mitigated but many architectural, mechanical, and electrical systems	Equipment and contents are generally secure, but may not operate due to mechanical	Negligible damage occurs. Power and other utilities are available, possibly from

Steps of the pushover analysis procedures, First total gravity load (Dead load and 25% live load) is applied in a load controlled pushover analysis followed by lateral load pushover analyses using displacement control. An invariant parabolic load pattern similar to IS 1893:2002 equivalents static analyses is considered for all the pushover analyses carried out here. This chapter presents the results obtained from the pushover analyses and discusses the nonlinear behaviour of the two selected buildings with and without shear hinges respectively.

4.2 Shear Hinge Properties For Frames

Shear hinge properties for individual beams and columns are calculated as per the procedure given in previous chapter.

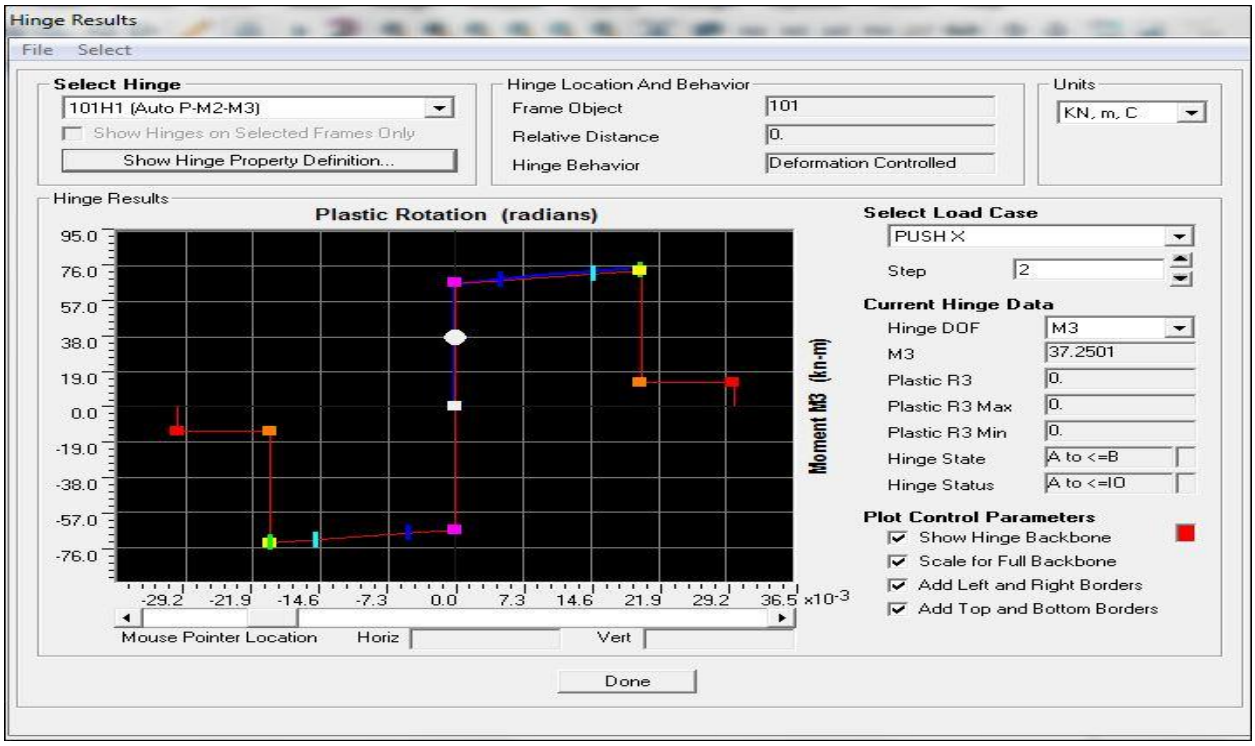

Fig: 4.2 Hinge properties definition

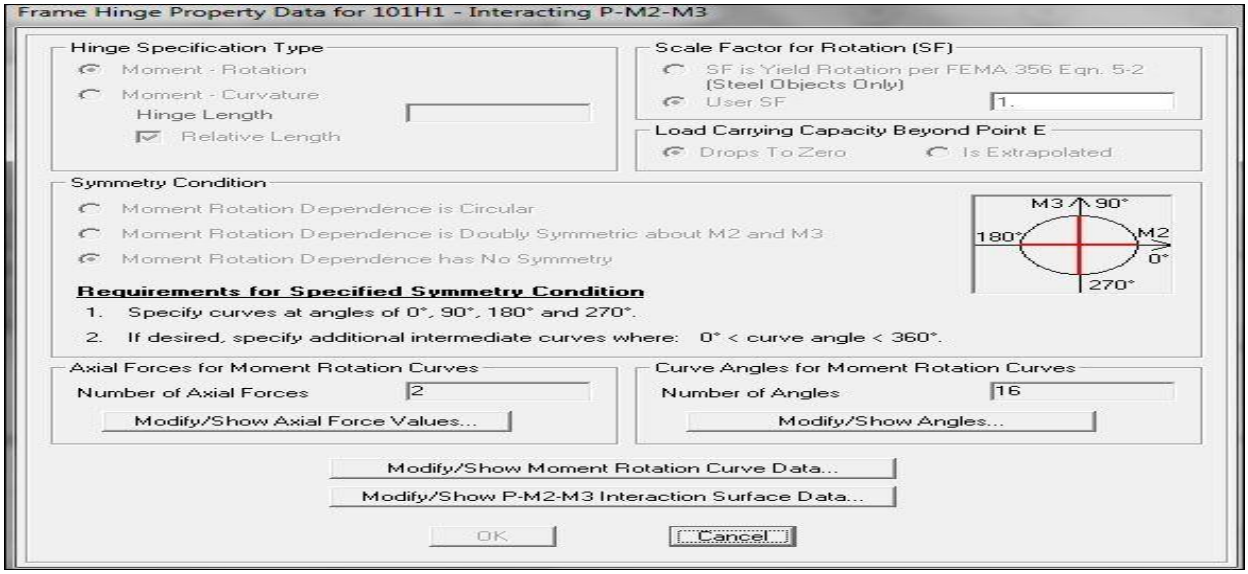

Fig: 4.3 Frame hinge property for interacting P-M2-M3 at a hinge

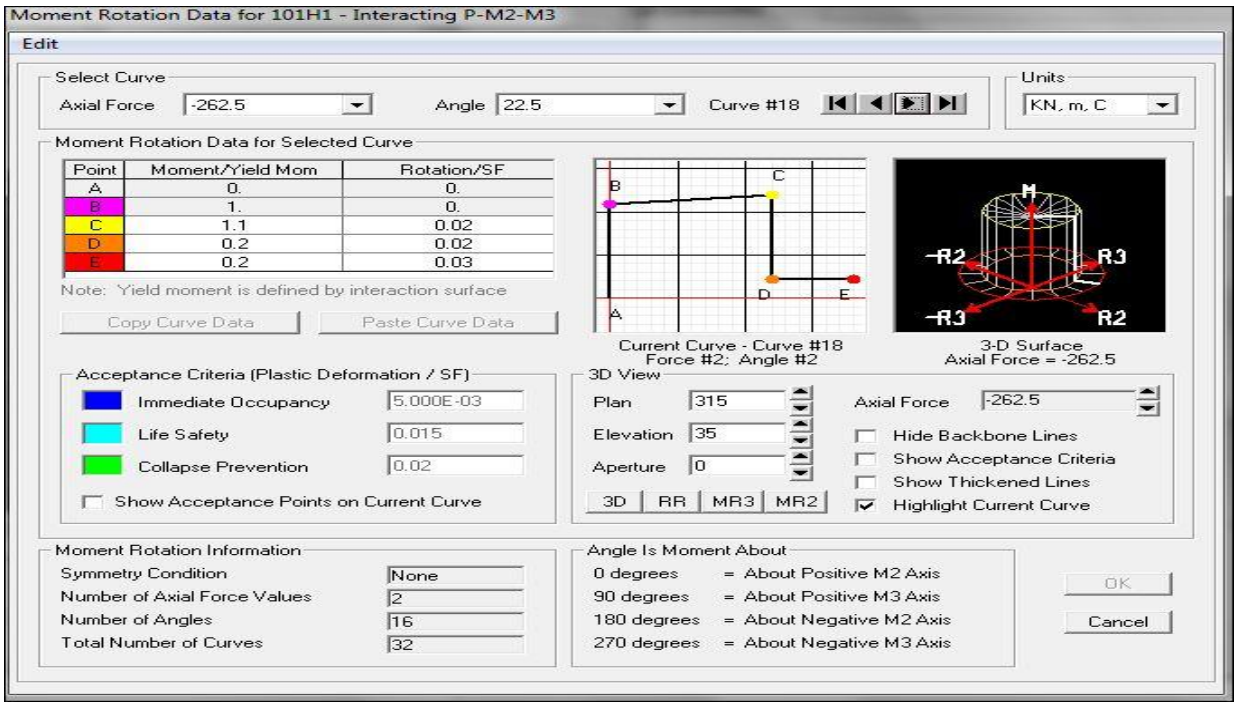

Fig: 4.4 Moment rotation curve for interacting P-M2-M3 at a hinge

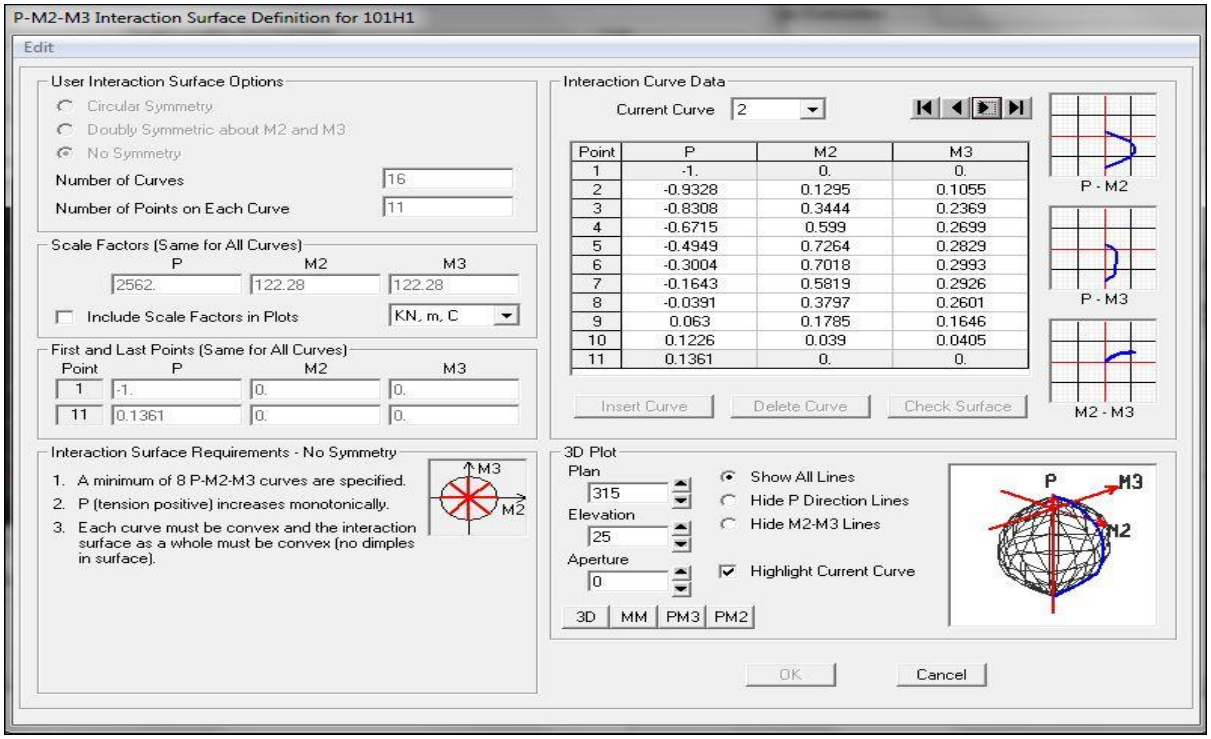

Fig: 4.5 Interaction surface definition at a hinge.

4.3 Capacity Curves For Pushover

The two resulting capacity curves for Push X and for Push Y analysis are plotted in Figs. and , respectively. Two building models with and without shear are considered. They are initially linear but start to deviate from linearity as the beams and the columns undergo inelastic deformation. When the buildings are pushed well into the inelastic range, the curves become linear again but with a smaller slope. The two curves could be approximated by a bilinear relationship.

In pushover analysis, the behaviour of the structure is depends upon the capacity curve that represents the relationship between the base shear force and the roof displacement. Due to this convenient representation in practice engineer can be visualized easily. It is observed that roof displacement was used for the capacity curve because it is widely accepted in practice. Two models of the selected building one with shear hinges and other without shear hinges are analysed in the present study.

1. Considering Flexural Hinges only.

2. Considering both Flexural and Shear Hinges

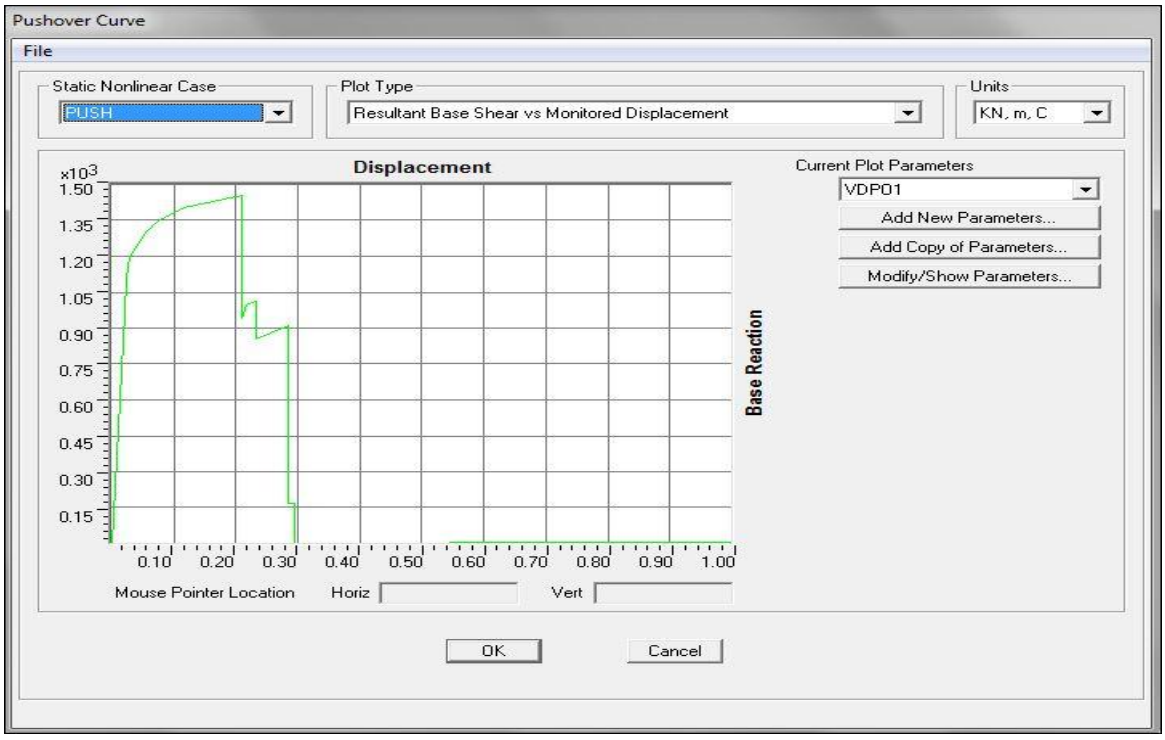

Fig: 4.6 Base shear Vs displacement curve for push (flexural case)

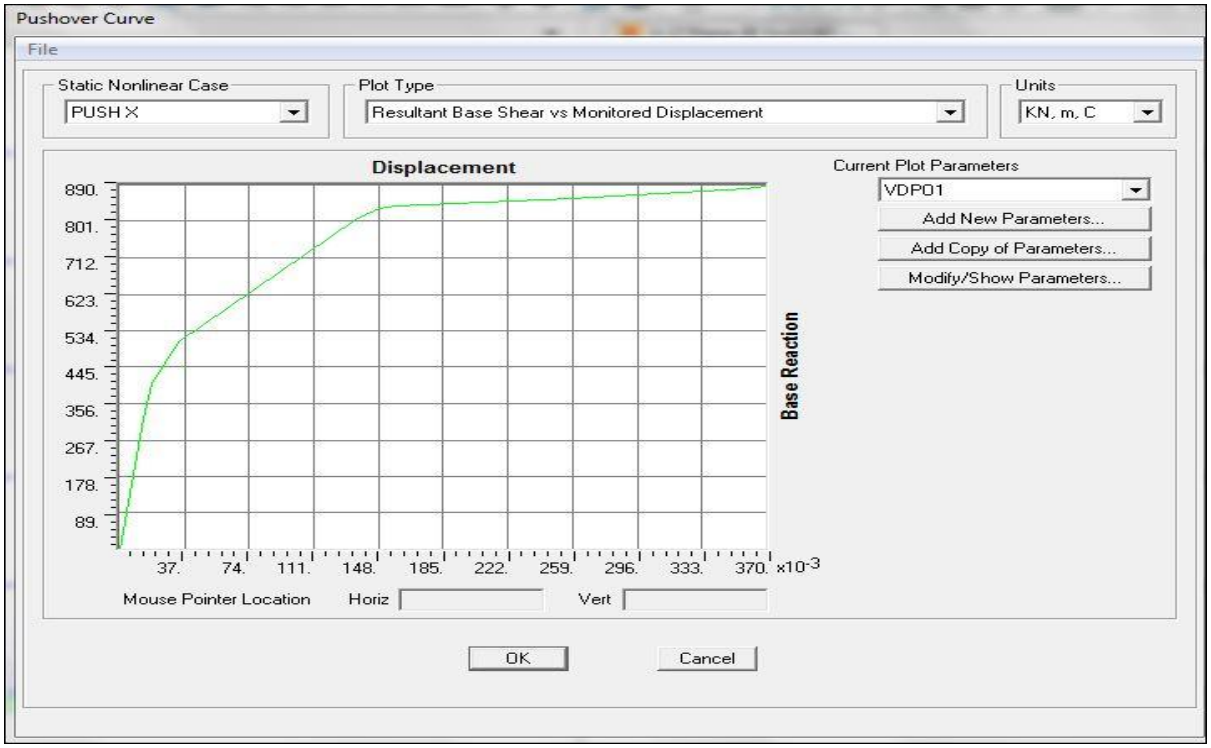

Fig: 4.7 Base shear Vs displacement curve for push (shear case)

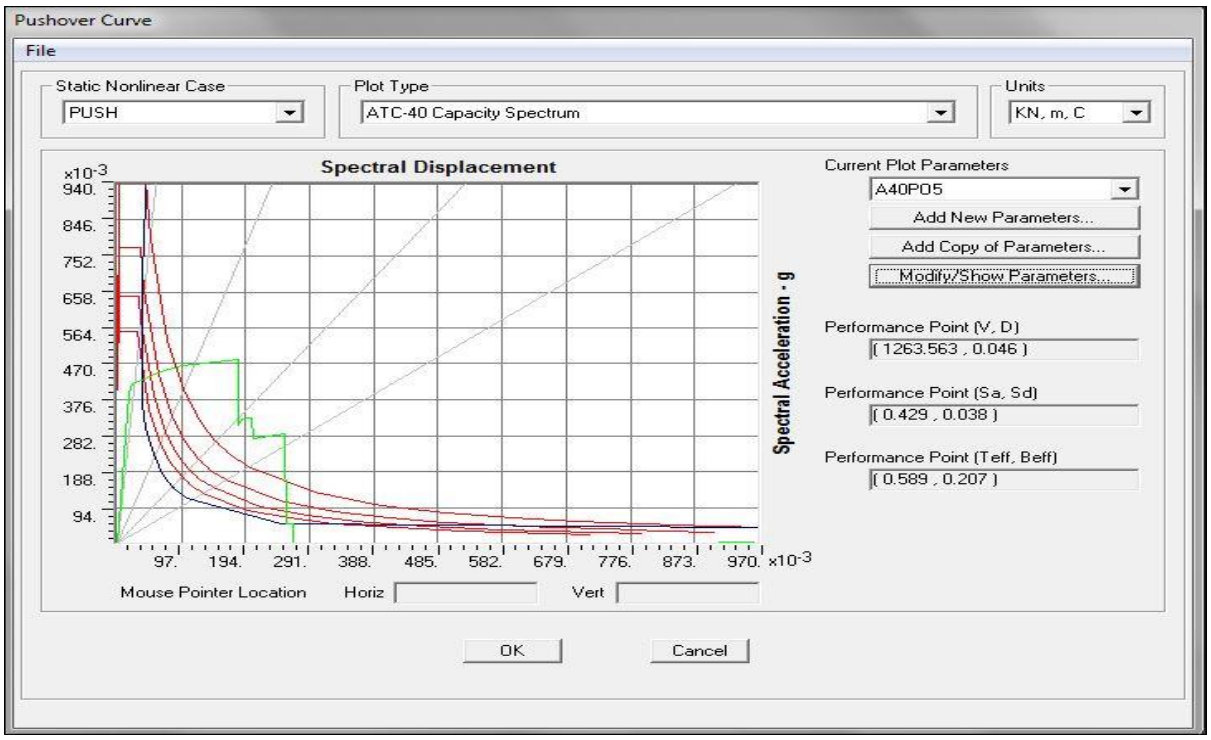

Fig: 4.8 ATC-40 Capacity Spectrum curve (flexural case)

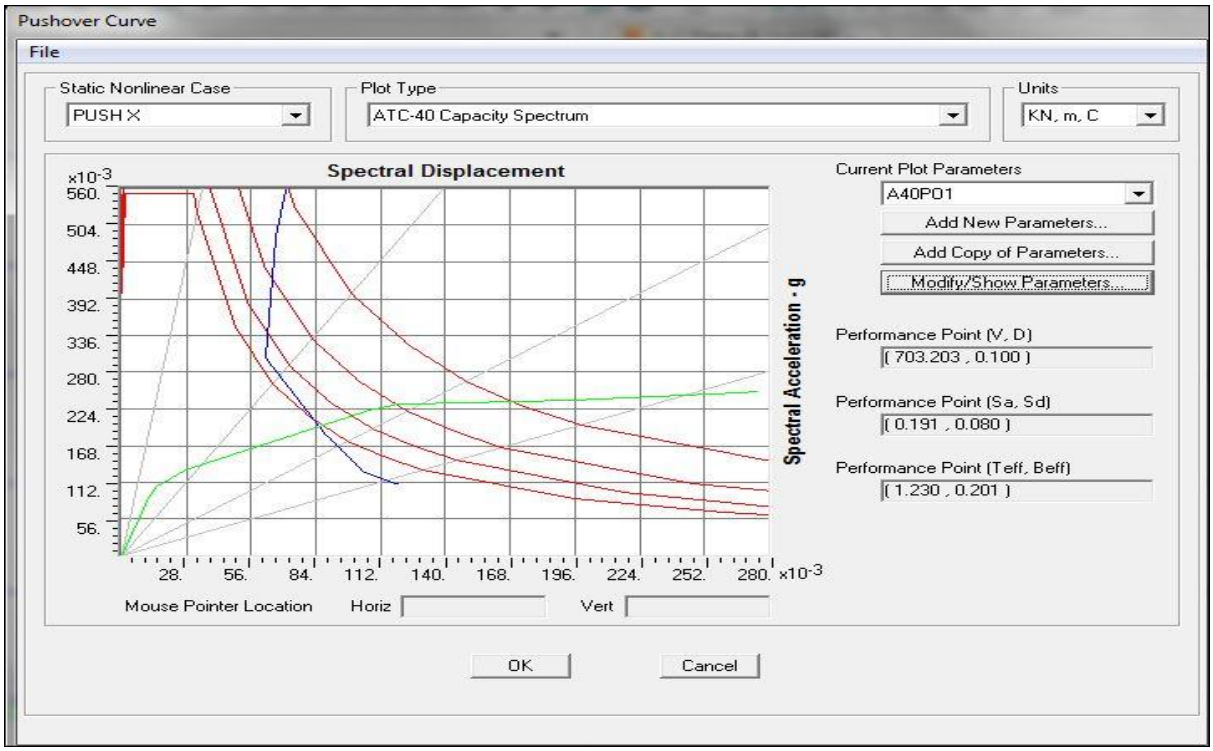

Fig: 4.9 ATC-40 Capacity Spectrum curve (shear case)

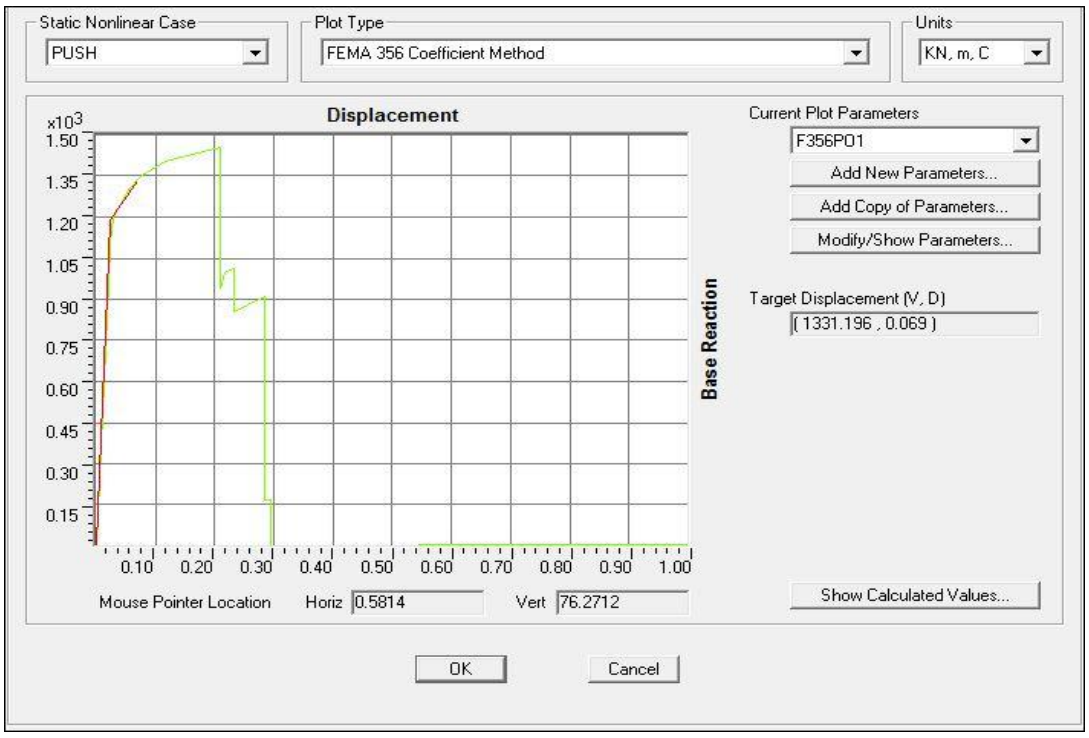

Fig: 4.10 FEMA 356 Coefficient Method Curve (flexural case)

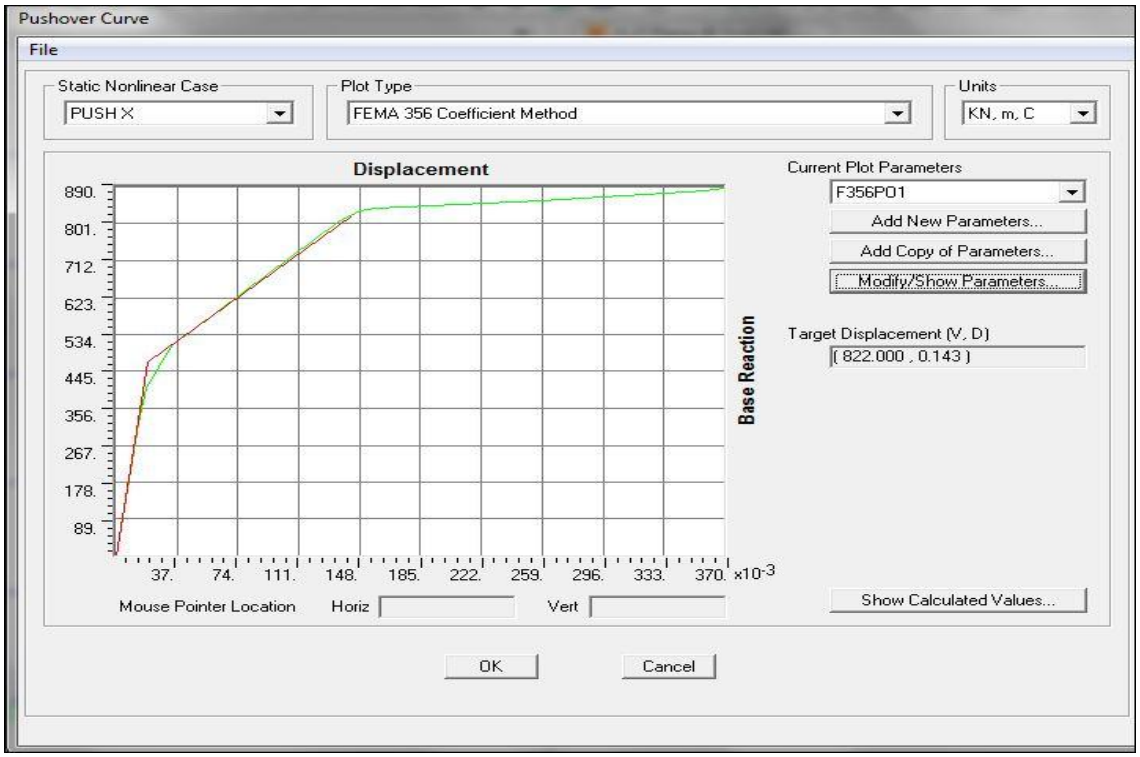

Fig: 4.11 FEMA 356 Coefficient Method Curve (shear case)

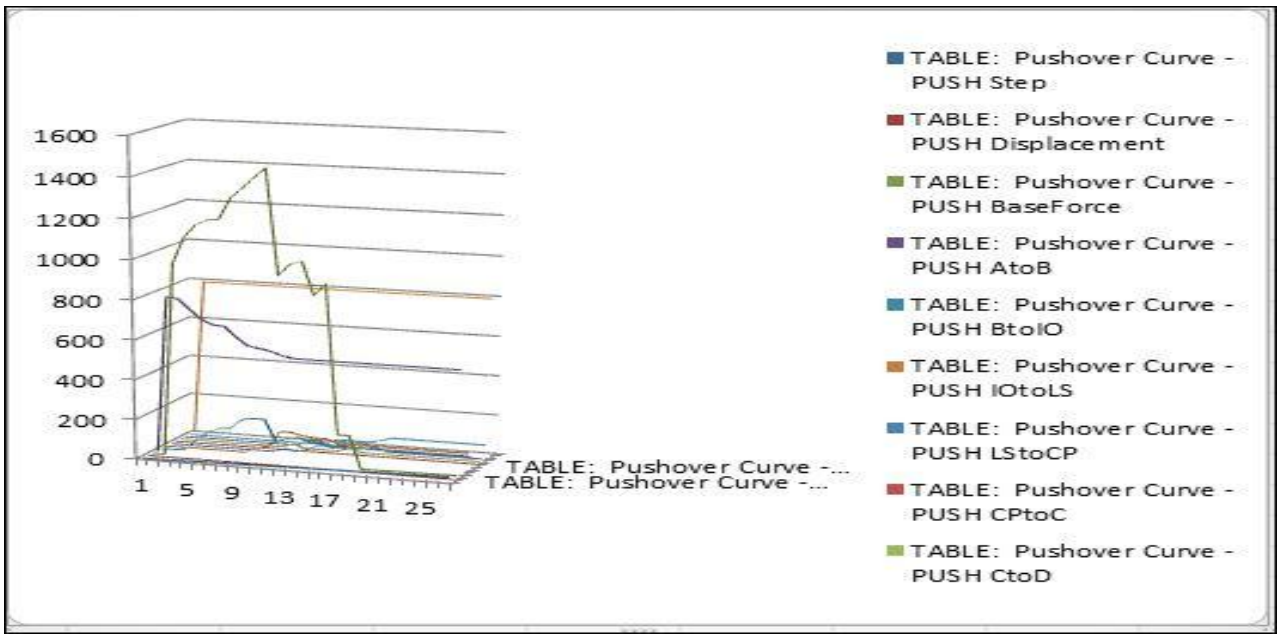

Fig: 4.12 Pushover curve (flexural case)

Table-4.2 Pushover curve Demand Capacity ATC-40

Table Display

File Edit

Pushover Curve Demand Capacity - ATC40 - PUSH

Step	Teff	Beff	SdCapacity	SaCapacity	SdDemand	SaDemand	Alpha	PFPhi
			m		m			
0	0.429288	0.050000	0.000000	0.000000	0.042655	0.931775	1.000000	1.000000
1	0.429288	0.050000	0.015668	0.342269	0.042655	0.931775	0.808295	1.262647
2	0.432946	0.056318	0.018114	0.389023	0.041750	0.896657	0.810066	1.260712
3	0.445167	0.077364	0.020149	0.409304	0.039439	0.801152	0.814103	1.254699
4	0.463725	0.107191	0.022265	0.416815	0.037349	0.699197	0.818488	1.247134
5	0.468631	0.114700	0.022774	0.417467	0.036961	0.677515	0.820046	1.245335
6	0.654312	0.257736	0.046215	0.434559	0.038526	0.362265	0.858173	1.198018
7	0.764406	0.275701	0.065344	0.450191	0.043737	0.301328	0.859846	1.193550
8	0.919794	0.287699	0.098089	0.466743	0.051660	0.245819	0.862637	1.180970
9	1.231379	0.317729	0.181820	0.482722	0.068517	0.181910	0.864139	1.157853
10	1.546615	0.659603	0.183187	0.308297	0.086058	0.144832	0.873541	1.149267
11	1.527041	0.600750	0.188880	0.326079	0.084969	0.146689	0.876192	1.148521
12	1.581896	0.580450	0.203818	0.327889	0.088021	0.141602	0.886299	1.144001
13	1.730063	0.747231	0.204346	0.274842	0.096266	0.129475	0.888795	1.141093
14	1.883039	0.640606	0.252685	0.286880	0.104778	0.118957	0.909486	1.125935
15	4.456286	4.805337	0.256010	0.051898	0.247960	0.050266	0.917636	1.111350
16	4.535266	4.669670	0.264681	0.051803	0.252355	0.049391	0.919658	1.108812
17	67.310173	1085.30092	0.265481	0.000236	3.745326	0.003328	0.921193	1.105505
18	57.378893	421.12744	0.363291	0.000444	3.192722	0.003904	0.933933	1.083128
19	53.413068	225.62772	0.462007	0.000652	2.972052	0.004194	0.939422	1.068145
20	51.263155	140.87997	0.561143	0.000860	2.852425	0.004370	0.942274	1.057647
21	49.911130	96.389540	0.660507	0.001067	2.777195	0.004488	0.943943	1.049938
22	48.981431	70.118590	0.760008	0.001275	2.725464	0.004573	0.945004	1.044056
23	48.302580	53.307208	0.859600	0.001483	2.687691	0.004637	0.945721	1.039427
24	47.784983	41.898533	0.959252	0.001691	2.658890	0.004688	0.946228	1.035693
25	47.755519	41.286808	0.965741	0.001705	2.657251	0.004691	0.946255	1.035475

Current Sort String

Current Filter String

Done

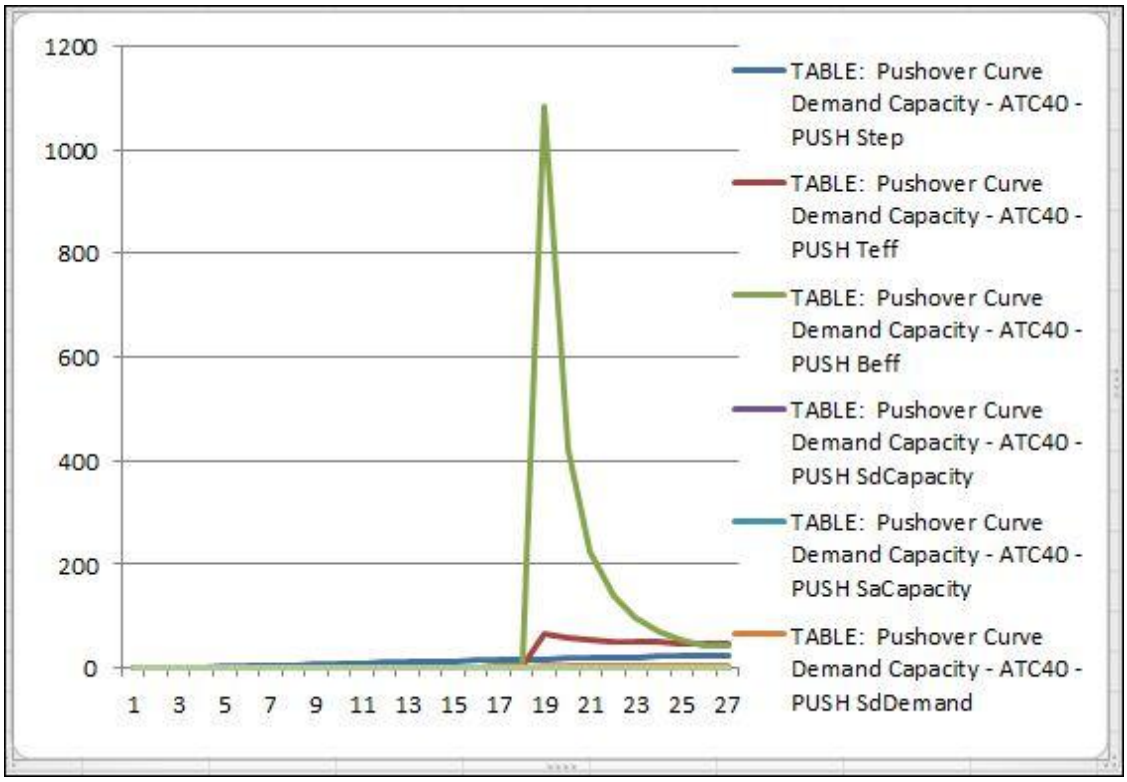

Fig: 4.13 Pushover curve for Demand Capacity (ATC-40)

4.4 Summary

This chapter presents the results obtained from pushover analysis of the selected building modes. Analyses were carried out for two building models, one without shear hinges and other with shear hinges, and for two orthogonal lateral directions (X and Y) of the model. The results presented here shows that the analysis can grossly overestimate the base shear and maximum roof displacement capacity of a building if the model ignores shear hinges. Also, estimated ductility ratio is found to be very high for the selected building model that does not consider shear hinge. These results demonstrate the importance of shear hinge in as seismic evaluation problem

CHAPTER 5.

RESULTS AND DISCUSSIONS

5.1 Base Reactions

Table-5.1 Base Reactions

OutputCase	CaseType	StepType	GlobalFX	GlobalFY	GlobalFZ	GlobalMX	GlobalMY	GlobalMZ
			KN	KN	KN	KN-m	KN-m	KN-m
DEAD	Non Static	Max	3.376E-13	-3.659E-13	2560.806	16542.8073	16542.8073	-5.612E-12
DEAD	Non Static	Min	3.376E-13	-3.659E-13	2560.806	16542.8073	16542.8073	-5.612E-12
PUSH X	Non Static	Max	3.376E-13	-1.359E-13	2560.814	16542.8556	16542.8073	-5399.4260
PUSH X	Non Static	Min	-835.824	-7.933E-13	2560.806	16542.8073	24664.8898	-5.612E-12
PUSH Y	Non Static	Max	3.376E-13	-2282.263	3097.877	20310.9480	16542.8073	-14743.482
PUSH Y	Non Static	Min	-9.011E-03	-1533.984	2560.806	11089.1105	20012.6144	-9909.5370

5.2 Joint Reactions

Table-5.2 Joint Reactions

Joint	Output Case	Case Type	Step Type	F1	F2	F3	M1	M2
				KN	KN	KN	KN-m	KN-m
1	DEAD	NonStatic	Max	0.283	0.259	81.336	-0.3017	0.3291
1	DEAD	NonStatic	Min	0.283	0.259	81.336	-0.3017	0.3291
1	PUSH X	NonStatic	Max	0.283	0.259	81.336	-0.1950	0.3291
1	PUSH X	NonStatic	Min	-28.314	0.193	-14.548	-0.3017	-66.1638
1	PUSH Y	NonStatic	Max	0.283	0.259	183.605	60.2121	0.3291
1	PUSH Y	NonStatic	Min	0.263	-219.701	39.111	-70.4921	0.2989
7	DEAD	NonStatic	Max	0.283	-5.678E-03	99.095	0.0054	0.3291
7	DEAD	NonStatic	Min	0.283	-5.678E-03	99.095	0.0054	0.3291
7	PUSH X	NonStatic	Max	0.283	-5.678E-03	99.095	0.0178	0.3291
7	PUSH X	NonStatic	Min	-28.866	-0.014	3.701	0.0054	-67.2876
7	PUSH Y	NonStatic	Max	0.286	42.993	170.317	21.2524	0.3315
7	PUSH Y	NonStatic	Min	0.282	-5.678E-03	98.172	-68.5861	0.3282
13	DEAD	NonStatic	Max	0.283	-5.573E-14	99.285	8.997E-14	0.3291
13	DEAD	NonStatic	Min	0.283	-5.573E-14	99.285	8.997E-14	0.3291
13	PUSH X	NonStatic	Max	0.283	9.242E-11	99.285	5.804E-10	0.3291
13	PUSH X	NonStatic	Min	-29.073	-2.934E-10	3.317	-4.699E-11	-67.6410
13	PUSH Y	NonStatic	Max	0.283	29.173	137.262	28.5621	0.3295
13	PUSH Y	NonStatic	Min	0.283	-19.892	98.205	-65.3972	0.3291
19	DEAD	NonStatic	Max	0.283	5.678E-03	99.095	-0.0054	0.3291
19	DEAD	NonStatic	Min	0.283	5.678E-03	99.095	-0.0054	0.3291
19	PUSH X	NonStatic	Max	0.283	0.014	99.095	-0.0054	0.3291
19	PUSH X	NonStatic	Min	-28.866	5.678E-03	3.701	-0.0178	-67.2876
19	PUSH Y	NonStatic	Max	0.289	10.690	102.425	25.6996	0.3374
19	PUSH Y	NonStatic	Min	0.283	-18.595	82.872	-60.0353	0.3289
25	DEAD	NonStatic	Max	0.283	-0.259	81.336	0.3017	0.3291
25	DEAD	NonStatic	Min	0.283	-0.259	81.336	0.3017	0.3291
25	PUSH X	NonStatic	Max	0.283	-0.193	81.336	0.3017	0.3291
25	PUSH X	NonStatic	Min	-28.314	-0.259	-14.548	0.1950	-66.1638
25	PUSH Y	NonStatic	Max	0.291	515.398	131.393	39.5225	0.3377
25	PUSH Y	NonStatic	Min	0.263	-56.140	-0.921	-56.5095	0.3129
31	DEAD	NonStatic	Max	8.652E-05	0.259	98.528	-0.3017	0.0018
31	DEAD	NonStatic	Min	8.652E-05	0.259	98.528	-0.3017	0.0018
31	PUSH X	NonStatic	Max	8.652E-05	0.260	103.015	-0.2257	0.0018
31	PUSH X	NonStatic	Min	-35.490	0.214	98.202	-0.3030	-80.4311

Table-5.2 Joint Reactions

Joint	Output Case	Case Type	Step Type	F1	F2	F3	M1	M2
				KN	KN	KN	KN-m	KN-m
31	PUSH Y	NonStatic	Max	8.652E-05	0.259	197.490	61.9436	0.0018
31	PUSH Y	NonStatic	Min	-0.017	-225.142	55.909	-71.0940	-0.0287
37	DEAD	NonStatic	Max	8.652E-05	-5.678E-03	116.287	0.0054	0.0018
37	DEAD	NonStatic	Min	8.652E-05	-5.678E-03	116.287	0.0054	0.0018
37	PUSH X	NonStatic	Max	8.652E-05	-5.276E-03	120.822	0.0089	0.0018
37	PUSH X	NonStatic	Min	-35.936	-9.325E-03	115.870	0.0045	-81.4749
37	PUSH Y	NonStatic	Max	8.652E-05	44.262	184.234	21.9050	0.0018
37	PUSH Y	NonStatic	Min	-2.245E-03	-5.678E-03	115.297	-69.9356	-0.0012
43	DEAD	NonStatic	Max	8.652E-05	-4.678E-14	116.477	8.065E-14	0.0018
43	DEAD	NonStatic	Min	8.652E-05	-4.678E-14	116.477	8.065E-14	0.0018
43	PUSH X	NonStatic	Max	8.652E-05	2.603E-11	121.032	2.959E-10	0.0018
43	PUSH X	NonStatic	Min	-36.152	-1.483E-10	116.031	-1.900E-11	-81.9721
43	PUSH Y	NonStatic	Max	8.652E-05	29.714	149.256	29.4650	0.0019
43	PUSH Y	NonStatic	Min	-4.278E-04	-20.570	115.367	-66.5606	0.0015
49	DEAD	NonStatic	Max	8.652E-05	5.678E-03	116.287	-0.0054	0.0018
49	DEAD	NonStatic	Min	8.652E-05	5.678E-03	116.287	-0.0054	0.0018
49	PUSH X	NonStatic	Max	8.652E-05	9.325E-03	120.822	-0.0045	0.0018
49	PUSH X	NonStatic	Min	-35.936	5.276E-03	115.870	-0.0089	-81.4749
49	PUSH Y	NonStatic	Max	5.992E-04	10.602	119.674	26.5134	0.0026
49	PUSH Y	NonStatic	Min	-1.462E-03	-19.121	98.659	-61.5984	0.0017
55	DEAD	NonStatic	Max	8.652E-05	-0.259	98.528	0.3017	0.0018
55	DEAD	NonStatic	Min	8.652E-05	-0.259	98.528	0.3017	0.0018
55	PUSH X	NonStatic	Max	8.652E-05	-0.214	103.015	0.3030	0.0018
55	PUSH X	NonStatic	Min	-35.490	-0.260	98.202	0.2257	-80.4311
55	PUSH Y	NonStatic	Max	6.087E-03	525.440	149.205	40.2455	0.0088
55	PUSH Y	NonStatic	Min	-0.014	-57.067	16.733	-57.9112	-0.0156
61	DEAD	NonStatic	Max	-7.218E-14	0.259	98.967	-0.3017	-1.171E-13
61	DEAD	NonStatic	Min	-7.218E-14	0.259	98.967	-0.3017	-1.171E-13
61	PUSH X	NonStatic	Max	-7.218E-14	0.260	99.072	-0.2252	-1.171E-13
61	PUSH X	NonStatic	Min	-35.361	0.214	98.587	-0.3019	-80.1313

Table-5.2 Joint Reactions

Joint	Output Case	Case Type	Step Type	F1	F2	F3	M1	M2
				KN	KN	KN	KN-m	KN-m
61	PUSH Y	NonStatic	Max	4.713E-11	0.259	201.722	62.5719	-1.171E-13
61	PUSH Y	NonStatic	Min	-1.100E-03	-227.224	56.249	-72.2335	-0.0016
67	DEAD	NonStatic	Max	-2.599E-14	-5.678E-03	116.726	0.0054	-4.854E-14
67	DEAD	NonStatic	Min	-2.599E-14	-5.678E-03	116.726	0.0054	-4.854E-14
67	PUSH X	NonStatic	Max	-2.599E-14	-5.678E-03	116.897	0.0099	-4.854E-14
67	PUSH X	NonStatic	Min	-35.851	-9.742E-03	115.874	0.0054	-81.2582
67	PUSH Y	NonStatic	Max	-2.599E-14	44.431	187.308	22.0399	-4.854E-14
67	PUSH Y	NonStatic	Min	-5.300E-04	-5.678E-03	115.660	-70.2334	-9.671E-04
73	DEAD	NonStatic	Max	-3.840E-14	-7.382E-14	116.916	1.071E-13	-5.354E-14
73	DEAD	NonStatic	Min	-3.840E-14	-7.382E-14	116.916	1.071E-13	-5.354E-14
73	PUSH X	NonStatic	Max	-3.840E-14	3.325E-12	116.952	8.462E-12	-5.354E-14
73	PUSH X	NonStatic	Min	-36.040	-3.834E-12	116.526	-6.689E-12	-81.7223
73	PUSH Y	NonStatic	Max	-3.840E-14	29.781	152.708	29.7103	-5.354E-14
73	PUSH Y	NonStatic	Min	-6.189E-05	-20.773	115.796	-66.8955	-9.447E-05
79	DEAD	NonStatic	Max	-4.108E-14	5.678E-03	116.726	-0.0054	-4.948E-14
79	DEAD	NonStatic	Min	-4.108E-14	5.678E-03	116.726	-0.0054	-4.948E-14
79	PUSH X	NonStatic	Max	-4.108E-14	9.742E-03	116.897	-0.0054	-4.948E-14
79	PUSH X	NonStatic	Min	-35.851	5.678E-03	115.874	-0.0099	-81.2582
79	PUSH Y	NonStatic	Max	5.519E-04	10.782	120.139	26.7014	9.489E-04
79	PUSH Y	NonStatic	Min	-4.344E-11	-19.319	99.702	-61.0527	-7.920E-11
85	DEAD	NonStatic	Max	-5.316E-15	-0.259	98.967	0.3017	-1.196E-14
85	DEAD	NonStatic	Min	-5.316E-15	-0.259	98.967	0.3017	-1.196E-14
85	PUSH X	NonStatic	Max	-5.316E-15	-0.214	99.072	0.3019	-1.196E-14
85	PUSH X	NonStatic	Min	-35.361	-0.260	98.587	0.2252	-80.1313

Table-5.2 Joint Reactions

Joint	Output Case	Case Type	Step Type	F1	F2	F3	M1	M2
				KN	KN	KN	KN-m	KN-m
85	PUSH Y	NonStatic	Max	4.531E-04	529.551	149.840	40.4470	0.0011
85	PUSH Y	NonStatic	Min	-7.468E-04	-57.482	17.321	-58.4657	-7.594E-11
91	DEAD	NonStatic	Max	-8.652E-05	0.259	98.528	-0.3017	-0.0018
91	DEAD	NonStatic	Min	-8.652E-05	0.259	98.528	-0.3017	-0.0018
91	PUSH X	NonStatic	Max	-8.652E-05	0.259	100.474	-0.2205	-0.0018
91	PUSH X	NonStatic	Min	-35.405	0.211	94.042	-0.3017	-80.4116
91	PUSH Y	NonStatic	Max	0.015	0.259	197.529	61.9368	0.0255
91	PUSH Y	NonStatic	Min	-8.652E-05	-225.138	55.904	-71.1035	-0.0018
97	DEAD	NonStatic	Max	-8.652E-05	-5.678E-03	116.287	0.0054	-0.0018
97	DEAD	NonStatic	Min	-8.652E-05	-5.678E-03	116.287	0.0054	-0.0018
97	PUSH X	NonStatic	Max	-8.652E-05	-5.678E-03	117.936	0.0122	-0.0018
97	PUSH X	NonStatic	Min	-35.788	-0.011	111.753	0.0054	-81.3128
97	PUSH Y	NonStatic	Max	1.393E-03	44.262	184.213	21.8986	-5.201E-04
97	PUSH Y	NonStatic	Min	-1.295E-04	-5.678E-03	115.297	-69.9337	-0.0030
103	DEAD	NonStatic	Max	-8.652E-05	-7.282E-14	116.477	1.072E-13	-0.0018
103	DEAD	NonStatic	Min	-8.652E-05	-7.282E-14	116.477	1.072E-13	-0.0018
103	PUSH X	NonStatic	Max	-8.652E-05	1.534E-10	118.513	1.976E-11	-0.0018
103	PUSH X	NonStatic	Min	-35.919	-2.663E-11	111.922	-3.068E-10	-81.7273
103	PUSH Y	NonStatic	Max	3.466E-04	29.717	149.309	29.4561	-0.0016
103	PUSH Y	NonStatic	Min	-1.115E-04	-20.564	115.367	-66.5658	-0.0020
109	DEAD	NonStatic	Max	-8.652E-05	5.678E-03	116.287	-0.0054	-0.0018
109	DEAD	NonStatic	Min	-8.652E-05	5.678E-03	116.287	-0.0054	-0.0018
109	PUSH X	NonStatic	Max	-8.652E-05	0.011	117.936	-0.0054	-0.0018
109	PUSH X	NonStatic	Min	-35.788	5.678E-03	111.753	-0.0122	-81.3128
109	PUSH Y	NonStatic	Max	2.098E-03	10.602	119.674	26.5112	-4.052E-04
109	PUSH Y	NonStatic	Min	-8.652E-05	-19.121	98.828	-61.6007	-0.0018

Table-5.2 Joint Reactions

Joint	Output Case	Case Type	Step Type	F1	F2	F3	M1	M2
				KN	KN	KN	KN-m	KN-m
115	DEAD	NonStatic	Max	-8.652E-05	-0.259	98.528	0.3017	-0.0018
115	DEAD	NonStatic	Min	-8.652E-05	-0.259	98.528	0.3017	-0.0018
115	PUSH X	NonStatic	Max	-8.652E-05	-0.211	100.474	0.3017	-0.0018
115	PUSH X	NonStatic	Min	-35.405	-0.259	94.042	0.2205	-80.4116
115	PUSH Y	NonStatic	Max	0.014	525.441	149.071	40.2414	0.0183
115	PUSH Y	NonStatic	Min	-4.753E-03	-57.066	16.599	-57.9112	-0.0061
121	DEAD	NonStatic	Max	-0.283	0.259	81.336	-0.3017	-0.3291
121	DEAD	NonStatic	Min	-0.283	0.259	81.336	-0.3017	-0.3291
121	PUSH X	NonStatic	Max	-0.283	0.263	175.214	-0.3017	-0.3291
121	PUSH X	NonStatic	Min	-34.193	0.259	81.336	-0.3098	-89.4355
121	PUSH Y	NonStatic	Max	-0.263	0.259	183.609	60.2120	-0.3018
121	PUSH Y	NonStatic	Min	-0.283	-219.701	39.110	-70.4930	-0.3291
127	DEAD	NonStatic	Max	-0.283	-5.678E-03	99.095	0.0054	-0.3291
127	DEAD	NonStatic	Min	-0.283	-5.678E-03	99.095	0.0054	-0.3291
127	PUSH X	NonStatic	Max	-0.283	-3.031E-03	193.089	0.0054	-0.3291
127	PUSH X	NonStatic	Min	-34.802	-5.678E-03	99.095	1.642E-04	-90.6290
127	PUSH Y	NonStatic	Max	-0.283	42.994	170.313	21.2527	-0.3290
127	PUSH Y	NonStatic	Min	-0.286	-5.678E-03	98.175	-68.5858	-0.3328
133	DEAD	NonStatic	Max	-0.283	-5.345E-14	99.285	9.126E-14	-0.3291
133	DEAD	NonStatic	Min	-0.283	-5.345E-14	99.285	9.126E-14	-0.3291
133	PUSH X	NonStatic	Max	-0.283	2.894E-10	193.420	1.701E-10	-0.3291
133	PUSH X	NonStatic	Min	-35.011	-8.657E-11	99.285	-5.825E-10	-91.0782
133	PUSH Y	NonStatic	Max	-0.283	29.173	137.261	28.5621	-0.3291
133	PUSH Y	NonStatic	Min	-0.283	-19.892	98.205	-65.3971	-0.3295
139	DEAD	NonStatic	Max	-0.283	5.678E-03	99.095	-0.0054	-0.3291
139	DEAD	NonStatic	Min	-0.283	5.678E-03	99.095	-0.0054	-0.3291
139	PUSH X	NonStatic	Max	-0.283	5.678E-03	193.089	-1.642E-04	-0.3291
139	PUSH X	NonStatic	Min	-34.802	3.031E-03	99.095	-0.0054	-90.6290
139	PUSH Y	NonStatic	Max	-0.283	10.690	102.425	25.7001	-0.3289
139	PUSH Y	NonStatic	Min	-0.288	-18.595	82.876	-60.0348	-0.3365

Table-5.2 Joint Reactions

Joint	Output Case	Case Type	Step Type	F1	F2	F3	M1	M2
				KN	KN	KN	KN-m	KN-m
145	DEAD	NonStatic	Max	-0.283	-0.259	81.336	0.3017	-0.3291
145	DEAD	NonStatic	Min	-0.283	-0.259	81.336	0.3017	-0.3291
145	PUSH X	NonStatic	Max	-0.283	-0.259	175.214	0.3098	-0.3291
145	PUSH X	NonStatic	Min	-34.193	-0.263	81.336	0.3017	-89.4355
145	PUSH Y	NonStatic	Max	-0.263	515.399	131.388	39.5227	-0.3102
145	PUSH Y	NonStatic	Min	-0.289	-56.140	-0.927	-56.5095	-0.3351

5.3 Capacity Curves for Push X and Push Y

The two resulting capacity curves for Push X and for Push Y analysis are plotted in Figs and, respectively. Two building models with and without shear are considered. When the building is pushed into the inelastic range, the curves become linear with a smaller slope. The two curves could be approximated by a bilinear relationship. Tables 6.3 and 6.4 presents the numerical data for capacity curves obtained from pushover analysis in X- and Y- directions respectively.

Table-5.3 Details of the Capacity Curves obtained from Push-X Analysis

Pushover Curve - PUSH X (WITHOUT SHEAR HINGE)		
Step	**Displacement**	**Base Force**
	m	**KN**
0	0	0
1	0.001379	416.61
2	0.001881	539.41
3	0.012236	580.84
4	0.023669	983.30
5	0.054329	1002.31
6	0.072882	1294.49
7	0.085077	1307.10
8	0.104477	1335.99
9	0.114615	1430.90
10	0.124492	1533.67
Pushover Curve - PUSH X (WITH SHEAR HINGE)		
Step	**Displacement**	**Base Force**
	m	**KN**
0	0	0
1	0.001347	320.97
2	0.001803	404.58
3	0.003344	508.00
4	0.013502	804.95
5	0.014851	832.18
6	0.015302	836.77
7	0.015808	839.29
8	0.025808	856.05
9	0.035808	882.15
10	0.036997	886.14

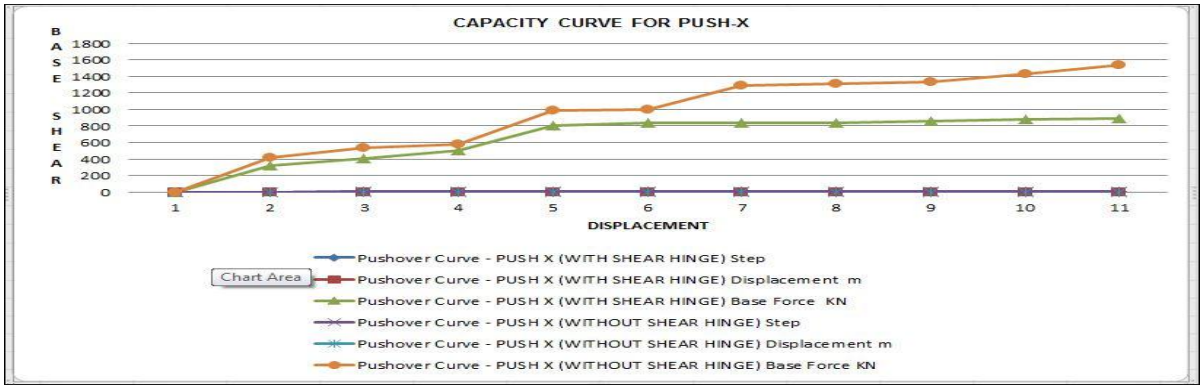

Fig: 5.1 Capacity curve for Push-X analysis.

Table-5.4 Details of the Capacity Curves obtained from Push-Y Analysis

Pushover Curve – PUSH Y (WITHOUT SHEAR HINGE)		
Step	Displacement	Base Force
	m	KN
0	0	0
1	0.000097	55.19
2	0.000136	249.44
3	0.000581	562.52
4	0.000668	690.23
5	0.000862	894.36
6	0.000956	1001.06
7	0.000990	1150.49

Pushover Curve - PUSH Y (WITH SHEAR HINGE)		
Step	Displacement	Base Force
	m	KN
0	0	0
1	0.000002	25.22
2	0.000093	106.48
3	0.000105	320.59
4	0.000125	393.70
5	0.000150	429.37
6	0.000235	526.47
7	0.000245	655.41
8	0.000391	778.72

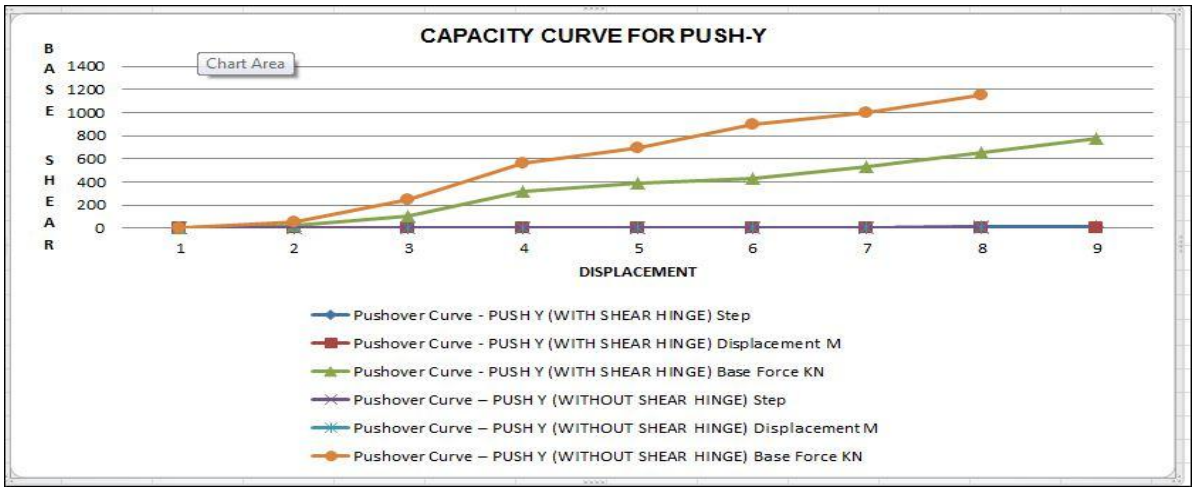

Fig: 5.2 Capacity curve for Push-X analysis.

Table-5.5 Summary of the base shear capacity and roof displacement of the building

	BASE SHEAR CAPACITY (kN)	ROOF DISPLACEMENT (mm)
Push -X analysis		
Without shear hinge	1042.46	59.5161
With shear hinge	717.18	14.9268
Overestimated percentage	45.35 %	298.72 %
Push -Y analysis		
Without shear hinge	657.61	0.6128
With shear hinge	404.50	0.1682
Overestimated percentage	62.57 %	264.32 %

Table presents the summary of the base shear capacity and roof displacement of the building as obtained from pushover analysis. Figs. 5.1 and 5.2 together with Table 5.5 clearly show how the pushover analysis overestimates the base shear capacity and roof displacement of the building when shear failure mode is not considered in the analysis. As per Table 5.5 pushover analysis overestimates base shear capacity of the building by approximately 45.35% in X-direction and 62.57% in Y-direction when shear hinges ignored. The maximum roof displacement capacity is overestimated by 298.72% in X-direction and 264.32% in Y-direction.

5.4 Plastic Hinge Mechanism

Sequences of plastic hinge formation are presented in Figs. 6.4 to 6.7. Performance levels of the plastic hinges are shown using colour code. The global yielding point corresponds to the displacement on the capacity curve where the system starts to soften. The ultimate point is considered at a displacement when lateral load capacity suddenly drops. Plastic hinges formation first occurs in beam ends and columns of lower stories, then extended to upper stories and continue with yielding of interior intermediate columns.

5.4.1 Flexural Hinge Formation for Push-X

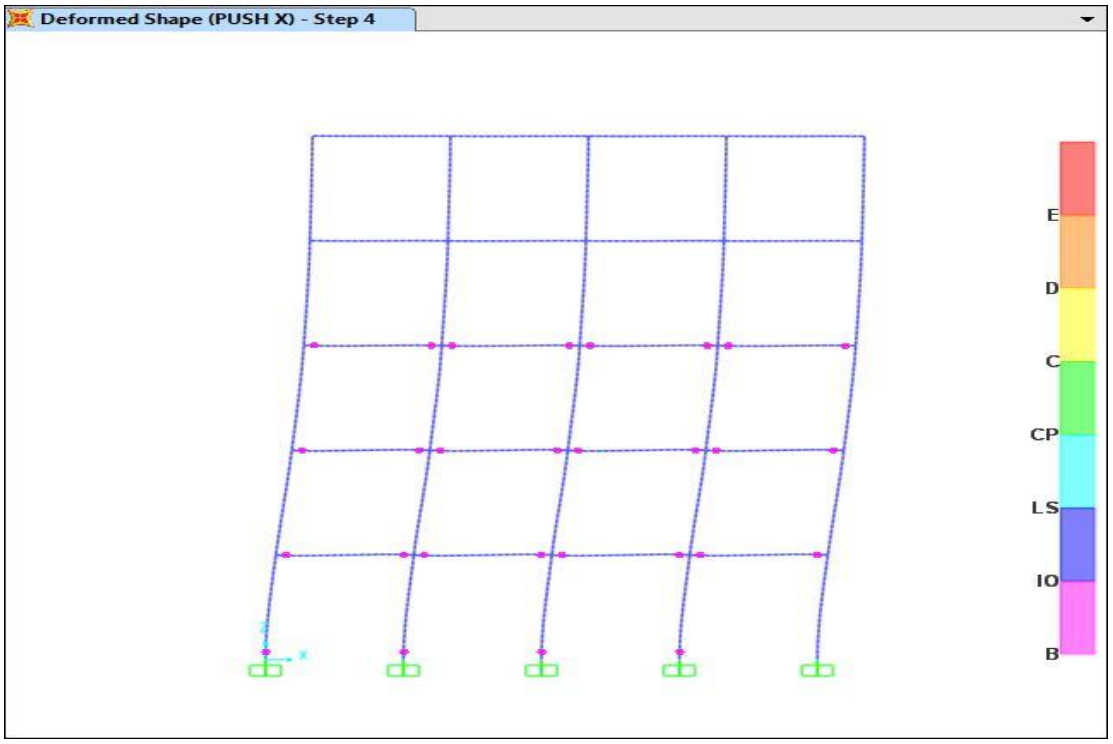

Fig: 5.3 flexural hinge deformed shape Push-X (at step 4)

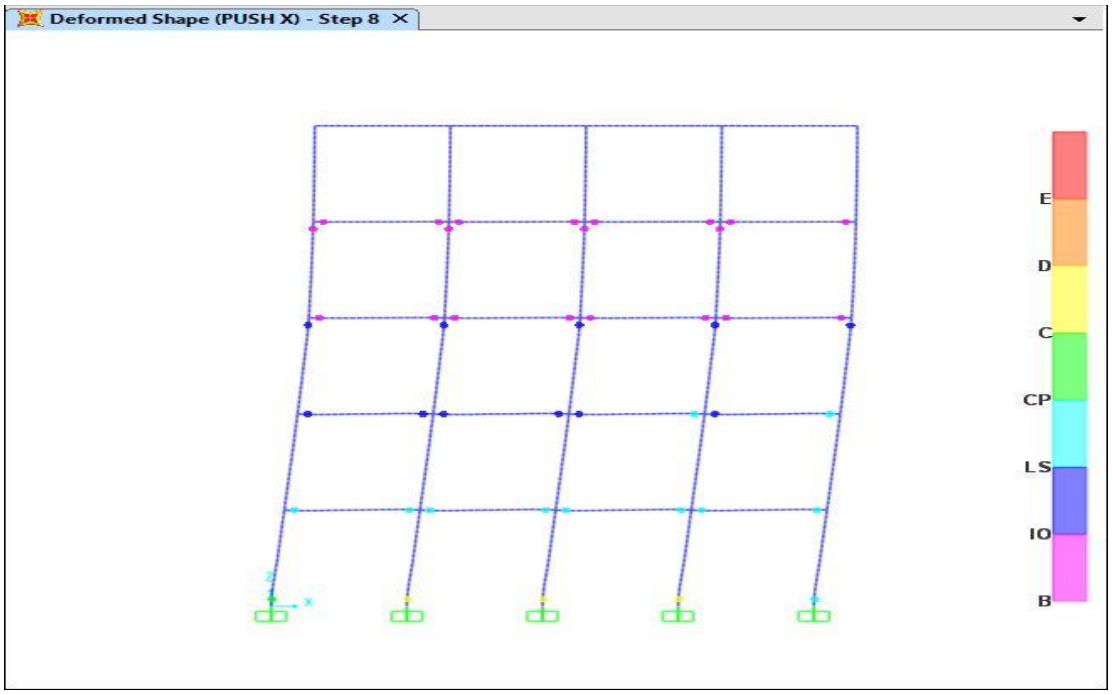

Fig: 5.4 flexural hinge deformed shape Push-X (at step 8)

5.4.2 Flexural Hinge Formation for Push-Y

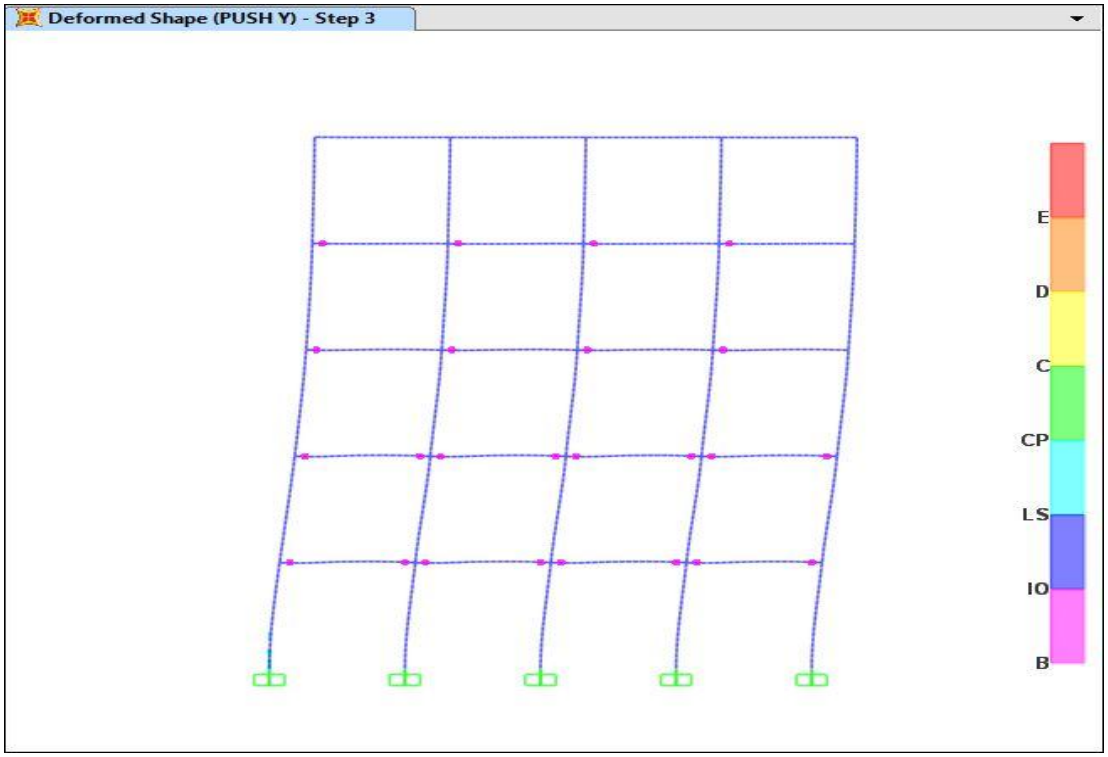

Fig: 5.5 flexural hinge deformed shape Push-Y (at step 3)

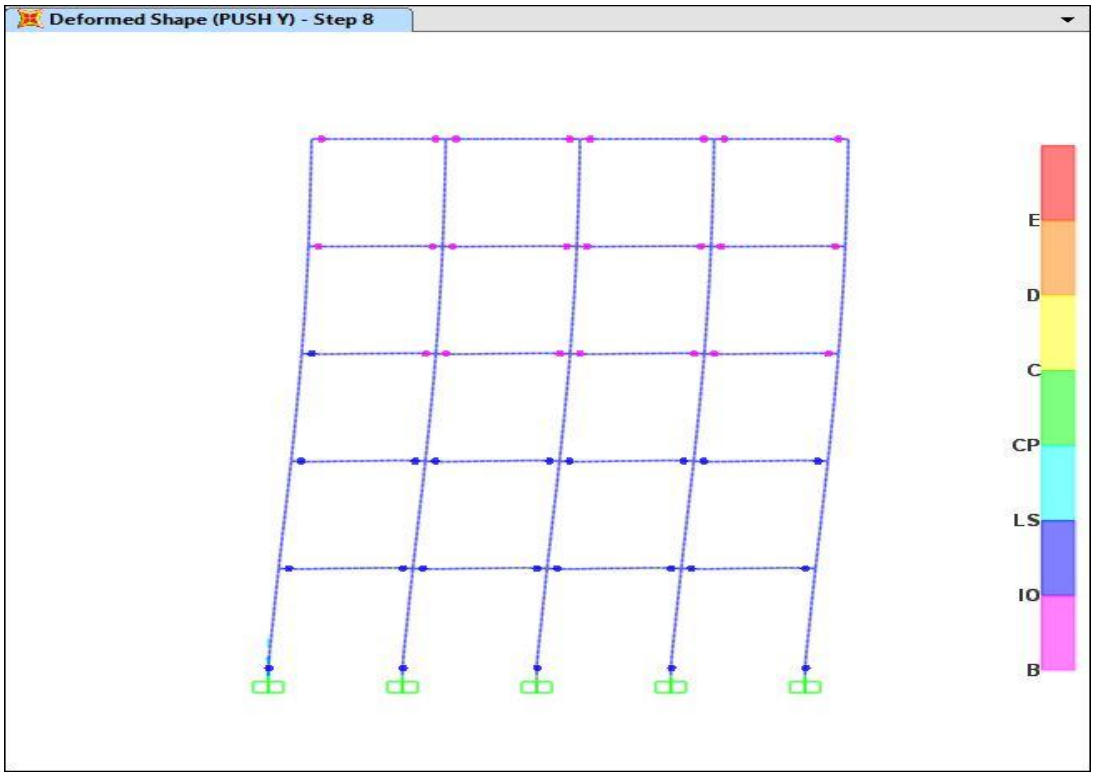

Fig: 5.6 flexural hinge deformed shape Push-Y (at step 8)

5.4.3 Shear Hinge Formation for Push-X

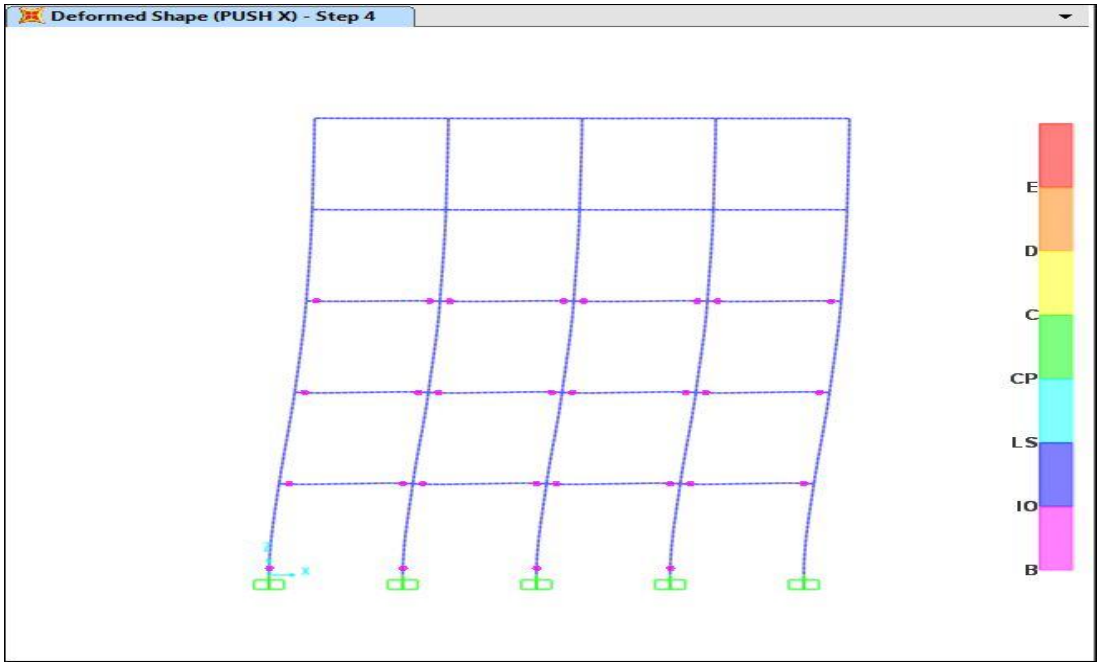

Fig: 5.7 shear hinge deformed shape Push-X (at step 4)

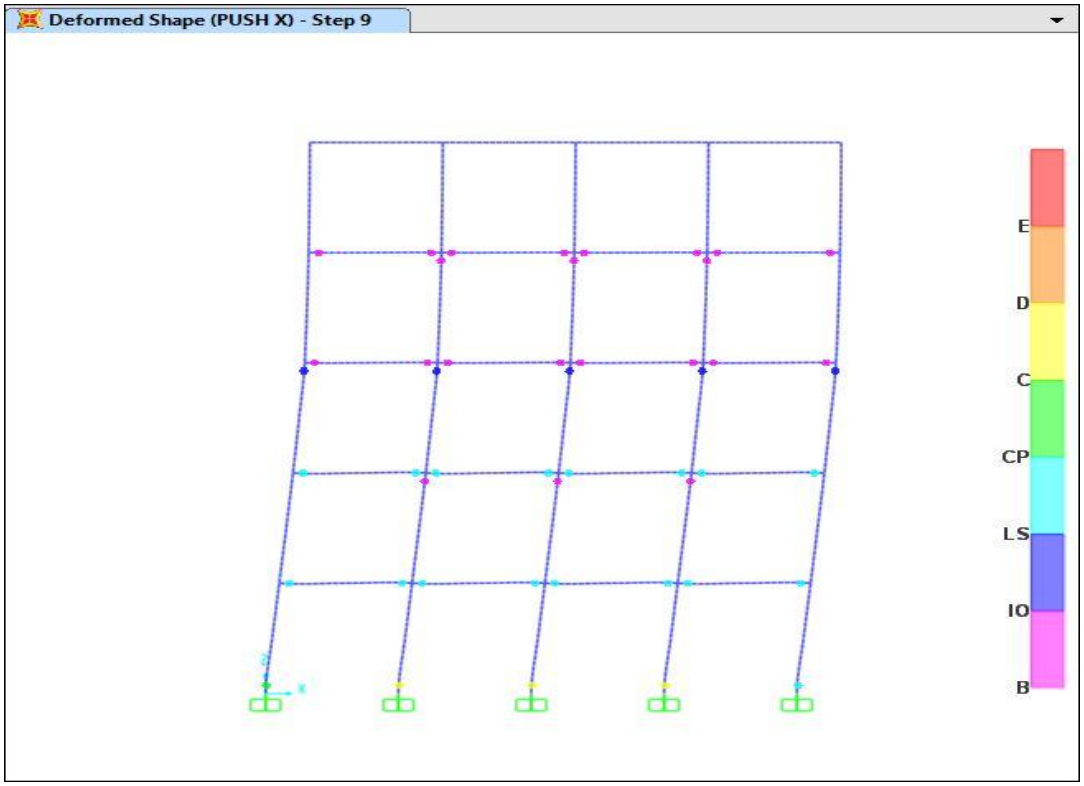

Fig: 5.8 shear hinge deformed shape Push-X (at step 9)

5.4.4 Shear Hinge Formation for Push-Y

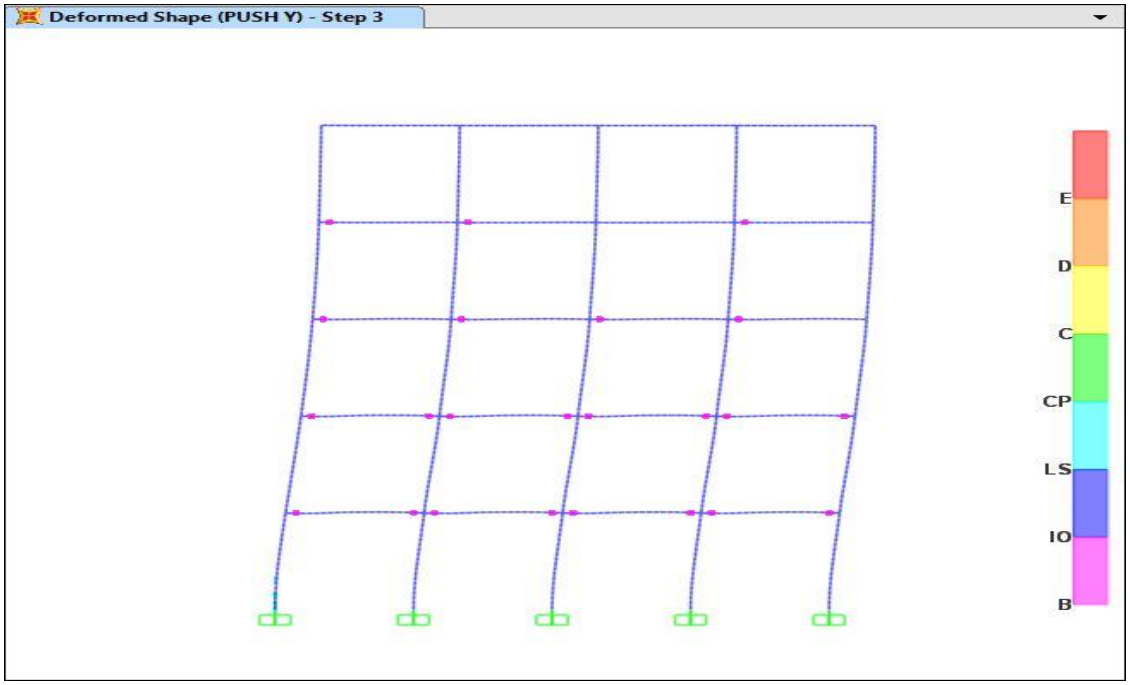

Fig: 5.9 shear hinge deformed shape Push-Y (at step 3)

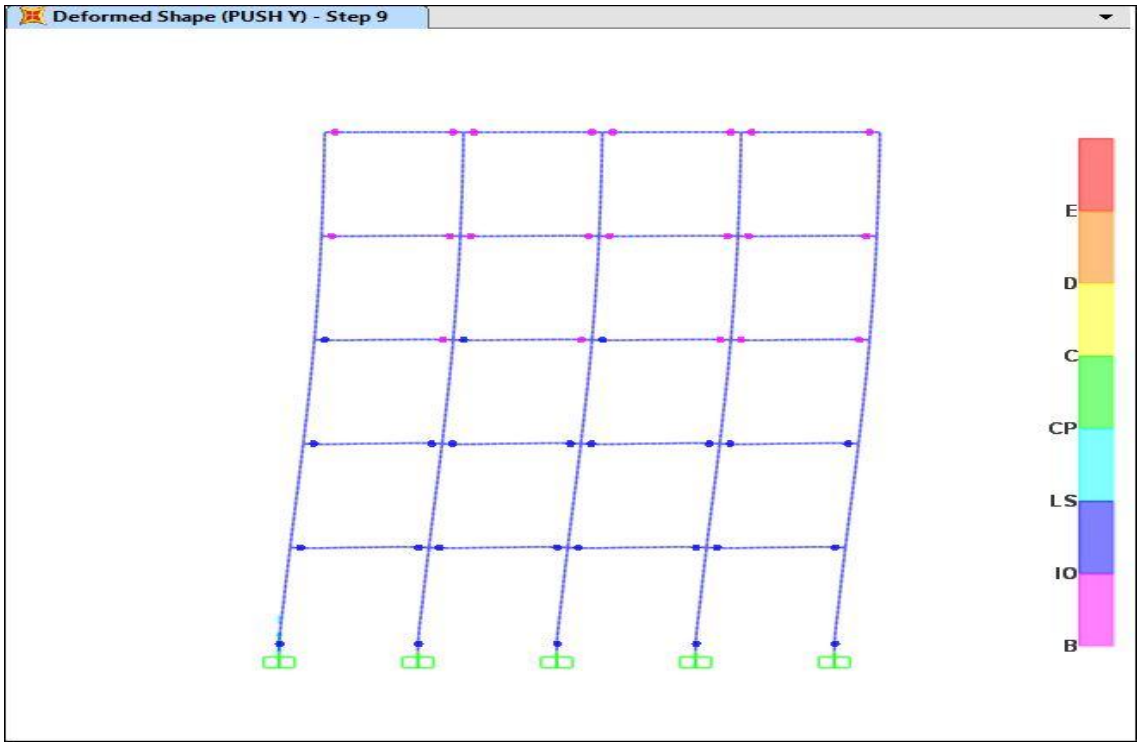

Fig: 5.10 shear hinge deformed shape Push-X (at step 9)

5.5 Summary

This chapter presents the results obtained from pushover analysis of the selected building model. Analyses were carried out for two building models, one without shear hinges and other with shear hinges, and for two orthogonal lateral directions (X and Y) of each model. The results presented here shows that the analysis can grossly overestimate the base shear capacity and maximum roof displacement of a building if the model ignores shear hinges. These results demonstrate the importance of shear hinge in as seismic evaluation problem.

CHAPTER 6.

CONCLUSIONS

The performance of reinforced concrete frames has been investigated by using the pushover analysis. There are the following conclusions drawn from the present study.

- The pushover analysis is a relatively simple way to explore the nonlinear behaviour of buildings.
- The behaviour of reinforced concrete frame building is indicated by the intersection of the demand and capacity curves and the distribution of Hinges in the beams and the columns.
- The results obtained in terms of capacity curves and plastic hinges gave an insight into the real behaviour of structures.
- The pushover analysis overestimates the base shear and roof displacement capacity of the building when shear failure mode is not considered in the analysis. As pushover analysis overestimates base shear capacity of the building by approximately 70% in X-direction and 45% in Y-direction when shear hinges ignored. The maximum roof displacement capacity is overestimated approximately by 300% in X-direction and 265% in Y-direction.

Followings are the salient conclusions for shear strength from the present study:

i) FEMA-356 does not consider contribution of concrete in shear strength calculation for beam under earthquake loading.

ii) Contribution of web reinforcement in shear strength given in IS-456: 2000 and ACI-318: 2008 represent ultimate shear strength.

iii) FEMA-356 consider ultimate shear strength carried by the web reinforcement (= strength of the beam) as 1.05 times the yield strength. But there is no engineering background for this consideration.

ANNEXURE –A

(NON LINEAR STATIC PUSHOVER ANALYSIS)

A.1 Introduction

The use of nonlinear static analysis (pushover analysis) came into practice in 1970's but the potential of the pushover analysis has been recognised for last 10-15 years. This procedure is mainly used to estimate the strength and drift capacity of existing structure and the seismic demand for this structure subjected to selected earthquake. This procedure can be used for checking the adequacy of new structural design as well. The effectiveness of pushover analysis and its computational simplicity brought this procedure into several seismic guidelines (ATC 40 and FEMA 356).

Pushover analysis is defined as an analysis where in a mathematical model directly incorporating the nonlinear load deformation characteristics of individual components and elements of the building shall be subjected to monotonically increasing lateral loads representing inertia forces in an earthquake until a target displacement exceeded. Target displacement is the maximum displacement (elastic plus inelastic) of the building at roof expected under selected earthquake ground motion. Pushover analysis assesses the structural performance by estimating the force and deformation capacity and seismic demand using a nonlinear static analysis algorithm. The seismic demand parameters are global displacements (at roof or any other reference point.), storey drifts, storey forces and component deformation and component forces. The analysis accounts for geometrical nonlinearity, material inelasticity and the redistribution of internal forces. Response characteristics that can be obtained from the pushover analysis are summarized as follows:

a) Estimates of forces and displacement capacities of the structures. Sequence of the member yielding and the progress of the overall capacity curve.
b) Estimates of the forces (axial, shear, moment) demands on potentially brittle elements and deformation demands on the ductile elements.
c) Estimates of the global displacement demand, corresponding inter-storey drifts and damages on structural and non-structural elements expected under the earthquake ground motion considered.

d) Sequences of the failure of elements and the consequent effect on the overall structural stability.
e) Identification of the critical regions, where the inelastic deformations are expected to be high and identification of strength irregularities (in plan and elevation) of the building.

Pushover analysis delivers all these benefits for an additional computational effort (modelling non linearity and change in analysis algorithm) over the linear static analysis.

A.2 Pushover Analysis Procedure

Pushover analysis is a static nonlinear procedure in which the magnitude of the lateral load is increased monotonically maintaining a predefined distribution pattern along the height of the building. Building is displaced till the control node reaches 'target displacement' or building collapses. The sequence of cracking, plastic hinging and failure of the structural components throughout the procedure is observed. The relation between base shear and control node is plotted for all the pushover analysis. Generation of base shear- control node displacement curve is single most important part of pushover analysis. This curve is conventionally called as pushover curve or capacity curve. This capacity curve is the basis of 'target displacement' estimation.

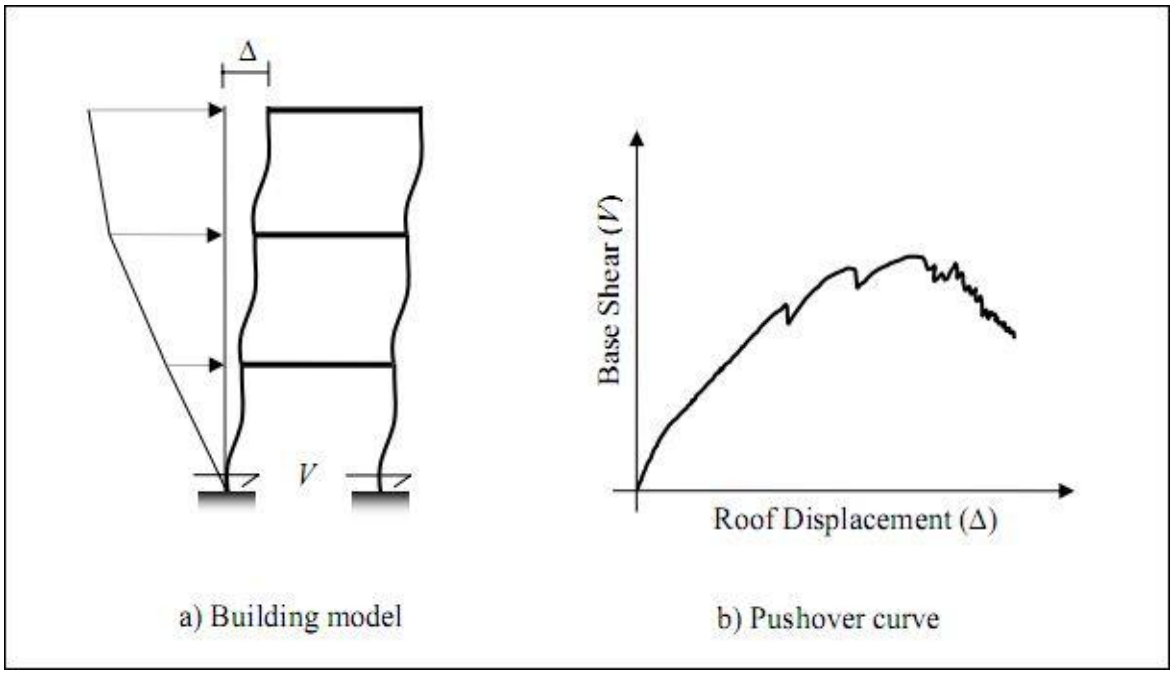

Fig: A.1 Schematic representation of pushover analysis procedure

So the pushover analysis may be carried out twice:

a) First time till the collapse of the building to estimate the target of the target displacement and
b) Next time till the target displacement to estimate the seismic demand. The seismic demands for the selected earthquake (storey drifts, storey forces and component deformation and forces) are calculated at target displacement level. The seismic demand is then compared with the corresponding structural capacity or predefined performance limit state to know what performance the structure will exhibit. Independent analysis along each of the two orthogonal principal axis of the building is permitted unless concurrent evaluation of bi-directional effects is required.

The analysis results are sensitive to the selection of the control node and selection of lateral load pattern. In general the centre of the mass location of the roof of the building is considered as control node. For selecting lateral load pattern in pushover analysis asset of guidelines as per FEMA 356 is explained. The lateral load is generally applied in both positive and negative directions in combination with gravity load (dead load and portion of the live load) to study the actual behaviour.

A.3 Lateral Load Profile

In pushover analysis the building is pushed with a specific load distribution pattern along the height of the building. The magnitude of the total force is increased but the pattern of the loading remains the same till the end of the process. Pushover analysis results (i.e. pushover curve, sequence of member yielding, building capacity and seismic demand) are very sensitive to the load pattern. The lateral load patterns should approximate the inertial forces expected in the building during an earthquake. The distribution of lateral inertial forces determines relative magnitudes of shears, moments and deformation within the structure. The distribution of these forces will vary continuously during earthquake response as the member yield and stiffness characteristics change. It also depends on the type and magnitude of earthquake ground motion. Although the inertia force distributions vary with the severity of the earthquake and with time, FEMA 356 recommends primarily invariant load pattern for pushover analysis of framed buildings.

Several investigations (Mwafy and Elnashai, 2000; Gupta and Kunnath, 2000) have found that a triangular or trapezoidal shape of the load provide a better fit to dynamic analysis results at the elastic range but at large deformations the dynamic envelopes are closer to the uniformly distributed force pattern. Since the constant distribution methods are incapable of capturing such variations in characteristics of the structural behaviour under earthquake loading, FEMA 356 suggests the use of at least two different patterns for all pushover analysis. Use of two different load pattern is intended to bind the range that may occur during actual dynamic response. FEMA 356 recommends selecting one load pattern from each of the following two groups:

Group – I:

i) Code based vertical distribution of lateral forces used in equivalent static analysis (permitted only when more than 75% of the total mass participates in the fundamental mode in the direction under consideration).
ii) A vertical distribution proportional to the shape of the fundamental mode in the direction under consideration (permitted only when more than 75% of the total mass participates in this mode).
iii) A vertical distribution proportional to the story shear distribution calculated by combining modal responses from a response spectrum analysis of the building (sufficient number of modes to capture at least 90% of the total building mass required to be considered). This distribution shall be used when the period of the fundamental mode exceeds 1.0 second.

Group – II:

i) A uniform distribution consisting of lateral forces at each level proportional to the total mass at each level.
ii) An adaptive load distribution that changes as the structure is displaced. The adaptive load distribution shall be modified from the original load distribution using a procedure that considers the properties of the yielded structure.

Instead of using the uniform distribution to bind the solution, FEMA 356 also allows adaptive lateral load patterns to be used but it does not elaborate the procedure. Although adaptive procedure may yield results that are more consistent with the characteristics of the building under consideration it requires considerably more

analysis effort. Figure shows the common lateral load pattern used in pushover analysis.

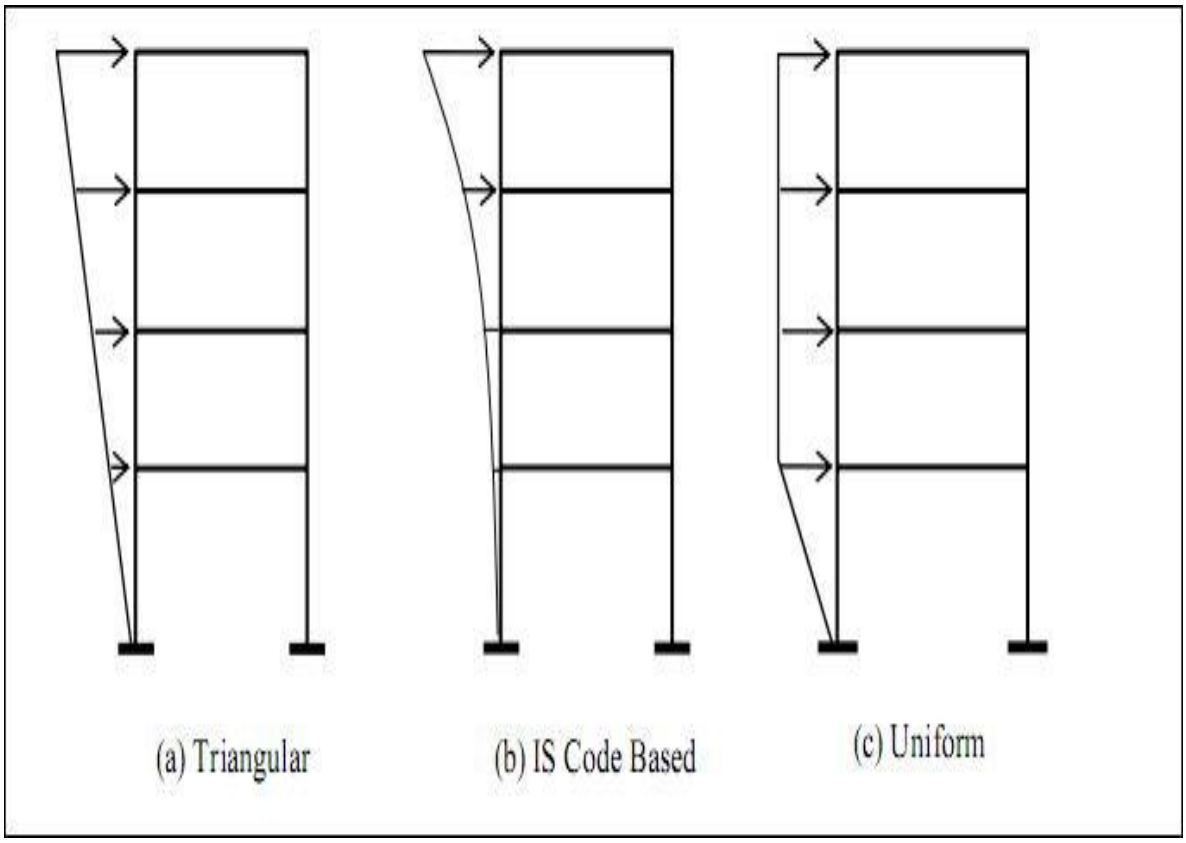

Fig: A.2 Lateral load pattern for pushover analysis as per FEMA 356

(Considering uniform mass distribution)

A.4 Target Displacement

Target displacement is the displacement demand for the building at the control node subjected to the ground motion under consideration. This is a very important parameter in pushover analysis because the global and component responses (forces and displacement) of the building at the target displacement are compared with the desired performance limit state to know the building performance. So the success of a pushover analysis largely depends on the accuracy of target displacement. There are two approaches to calculate target displacement:

(a) Displacement Coefficient Method (DCM) of FEMA 356 and

(b) Capacity Spectrum Method (CSM) of ATC 40.

Both of these approaches use pushover curve to calculate global displacement demand on the building from the response of an equivalent single degree of freedom (SDOF) system. The only difference in these two methods is the technique used.

A.4.1 Displacement Coefficient Method (FEMA 356)

This method primarily estimates the elastic displacement of an equivalent SDOF system assuming initial linear properties and damping for the ground motion excitation under consideration. Then it estimates the total maximum inelastic displacement response for the building at roof by multiplying with a set of displacement coefficients.

The process begins with the base shear versus roof displacement curve (pushover curve). An equivalent period (T_{eq}) is generated from initial period (T_i) by graphical procedure. This equivalent period represents the linear stiffness of the equivalent SDOF system. The peak elastic spectral displacement corresponding to this period is calculated directly from the response spectrum representing the seismic ground motion under consideration.

$$S_d = \frac{T_{eq}^2}{4\pi^2} S_a \qquad \text{…….. (A.1)}$$

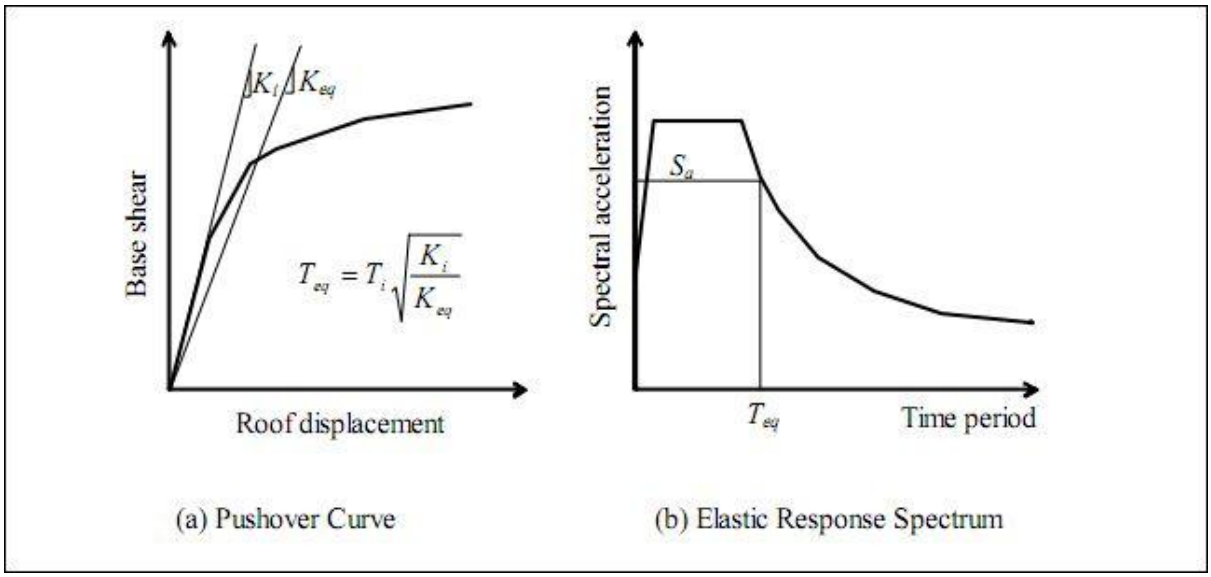

Fig: A.3 Schematic representation of Displacement Coefficient Method (FEMA 356)

Now, the expected maximum roof displacement of the building (target displacement) under the selected seismic ground motion can be expressed as:

$$\delta_t = C_0 C_1 C_2 C_3 S_d = C_0 C_1 C_2 C_3 \frac{T_{eq}^2}{4\pi^2} S_a \qquad \text{..... (A.2)}$$

Where,

C_0 = a shape factor (often taken as the first mode participation factor) to convert the spectral displacement of equivalent SDOF system to the displacement at the roof of the building.

C_1 = the ratio of expected displacement (elastic plus inelastic) for an inelastic system to the displacement of a linear system.

C_2 = a factor that accounts for the effect of pinching in load deformation relationship due to strength and stiffness degradation.

C_3 = a factor to adjust geometric nonlinearity (P-Δ) effects

These coefficients are derived empirically from statistical studies of the nonlinear response history analyses of SDOF systems of varying periods and strengths and given in FEMA 356.

A.4.2 Capacity Spectrum Method (ATC 40)

The basic assumption in Capacity Spectrum Method is also the same as the previous one. That is, the maximum inelastic deformation of a nonlinear SDOF system can be approximated from the maximum deformation of a linear elastic SDOF system with an equivalent period and damping. This procedure uses the estimates of ductility to calculate effective period and damping. This procedure uses the pushover curve in an acceleration displacement response spectrum (ADRS) format. This can be obtained through simple conversion using the dynamic properties of the system. The pushover curve in an ADRS format is termed a 'capacity spectrum' for the structure. The seismic ground motion is represented by a response spectrum in the same ADRS format and it is termed as demand spectrum.

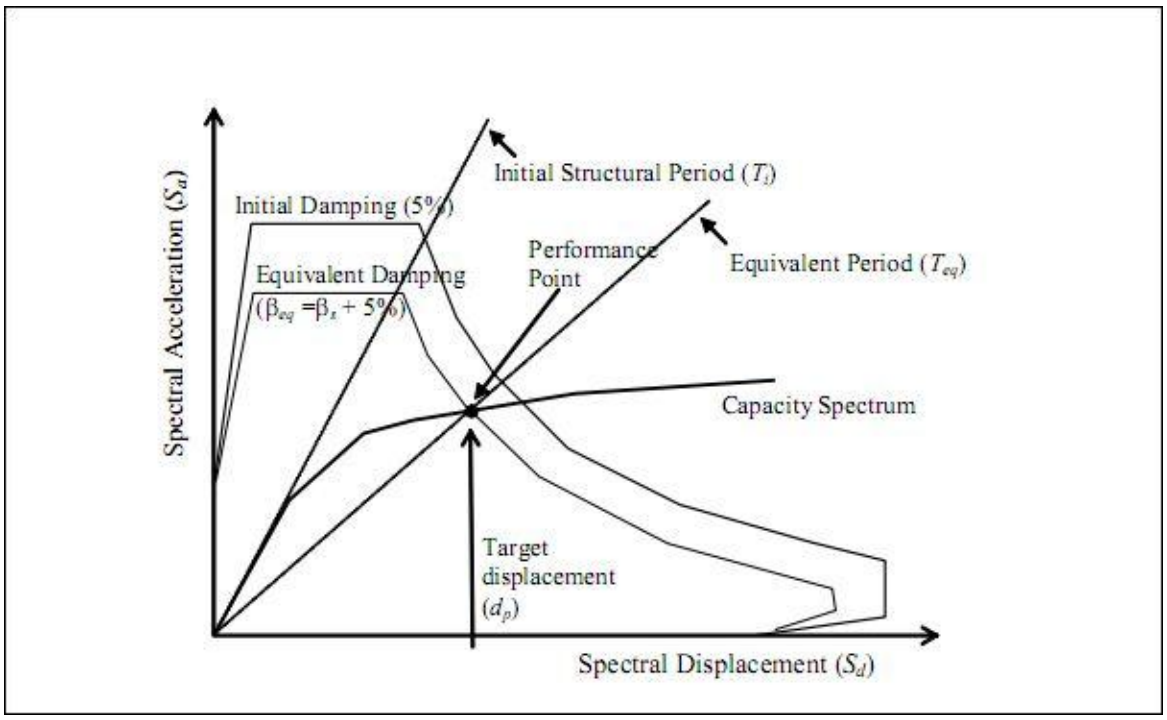

Fig: A.4 Schematic representation of Capacity Spectrum Method (ATC 40)

The equivalent period (T_{eq}) is computed from the initial period of vibration (T_i) of the nonlinear system and displacement ductility ratio (μ). Similarly, the equivalent damping ratio (β_{eq}) is computed from initial damping ratio (ATC 40 suggests an initial elastic viscous damping ratio of 0.05 for reinforced concrete building) and the

displacement ductility ratio (μ). ATC 40 provides the following equations to calculate equivalent time period (T_{eq}) and equivalent damping (β_{eq}).

$$T_{eq} = T_i \sqrt{\frac{\mu}{1+\alpha\mu-\alpha}} \qquad \text{..... (A.3)}$$

$$\beta_{eq} = \beta_i + k\frac{2(\mu-1)(1-\alpha)}{\pi\mu(1+\alpha\mu-\alpha)} = 0.05 + k\frac{2(\mu-1)(1-\alpha)}{\pi\mu(1+\alpha\mu-\alpha)} \qquad \text{.....(A.4)}$$

Where α is the post-yield stiffness ratio and μ is an adjustment factor to approximately account for changes in hysteretic behaviour in reinforced concrete structures.

ATC 40 relates effective damping to the hysteresis curve Fig. A.5 and proposes three hysteretic behaviour types that alter the equivalent damping level. Type A hysteretic behaviour is meant for new structures with reasonably full hysteretic loops, and the corresponding equivalent damping ratios take the maximum values. Type C hysteretic behaviour represents severely degraded hysteretic loops, resulting in the smallest equivalent damping ratios. Type B hysteretic behaviour is an intermediate hysteretic behaviour between types A and C. The value of μ decreases for degrading systems (hysteretic behaviour types B and C).

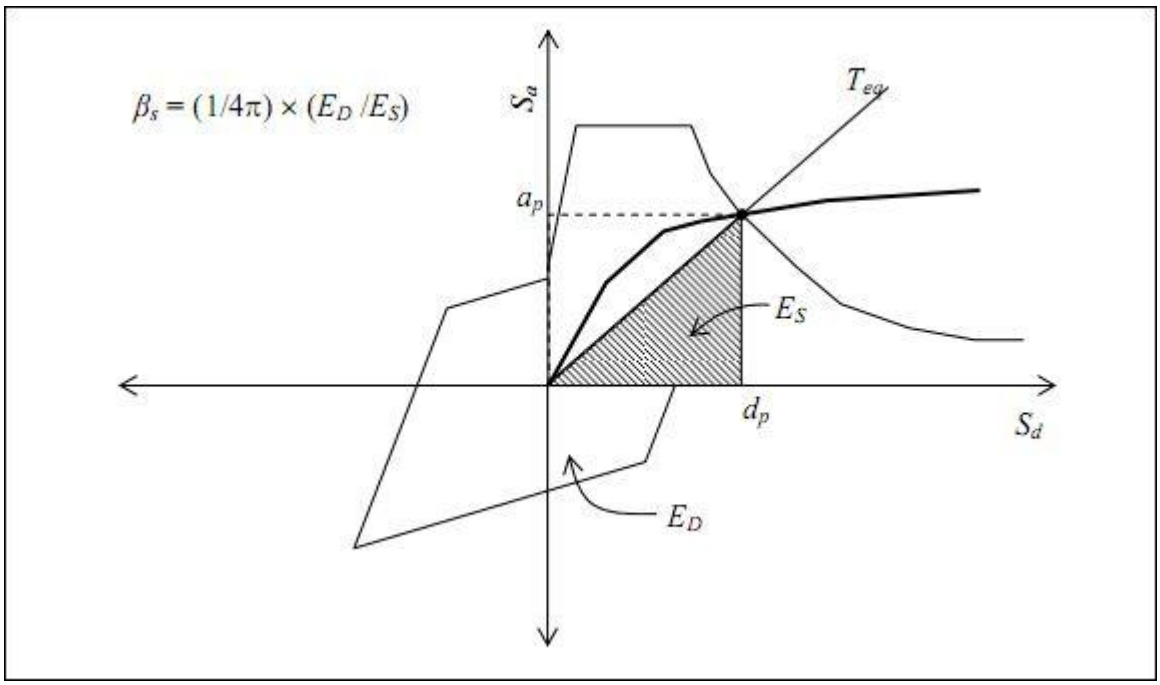

Fig: A.5 Effective damping in Capacity Spectrum Method (ATC 40)

The equivalent period in Eq. A.3 is based on a lateral stiffness of the equivalent system that is equal to the secant stiffness at the target displacement. This equation does not depend on the degrading characteristics of the hysteretic behaviour of the system. It only depends on the displacement ductility ratio (μ) and the post-yield stiffness ratio (α) of the inelastic system.

ATC 40 provides reduction factors to reduce spectral ordinates in the constant acceleration region and constant velocity region as a function of the effective damping ratio. The spectral reduction factors are given by:

$$SR_A = \frac{3.21 - 0.68 \ln(100\beta_{eq})}{2.2} \quad \text{..... (A.5)}$$

$$SR_V = \frac{2.31 - 0.41 \ln(100\beta_{eq})}{1.65} \quad \text{..... (A.6)}$$

Where,

SR_A is the spectral reduction factor to be applied to the constant acceleration region, and SR_V is the spectral reduction factor to be applied to the constant velocity region (descending branch) in the linear elastic spectrum. Since the equivalent period and

equivalent damping are both functions of the displacement ductility ratio, it is required to have prior knowledge of displacement ductility ratio. However, this is not known at the time of evaluating a structure. Therefore, iteration is required to determine target displacement. ATC 40 describes three iterative procedures with different merits and demerits to reach the solution.

REFERENCES

[1]. ATC 40, “Seismic evaluation and retrofit of concrete buildings Applied Technology Council”, 1996.

[2]. Federal Emergency Federal Agency, FEMA-356, “Prestandard and Commentary for Seismic Rehabilitation of Buildings”, Washington DC, 2000.

[3]. Chopra AK, Goel RK, Report No PEER 2001/03, “A modal pushover analysis procedure to estimate seismic demands for buildings: Theory and Preliminary evaluation”, Pacific Earthquake Engineering Research Centre, University of California, Berkeley, California. 2001

[4]. Fajfar P, Fishinger, 1988, M. N2-A, “Method for nonlinear seismic analysis of regular buildings”, Proc. 9th World Conference on Earthquake Engineering, Tokyo, 5:111-16.

[5]. Fajfar P, Gaperesic P, 1991, “The N2 method for the seismic damage analysis of RC buildings”, Journal of Earthquake Engineering and Structural Dynamics, 25:31-46.

[6]. CSI, SAP 2000, Ver. 10.07, “Integrated finite element analysis and design of structures basic analysis reference manual”, Berkeley (CA, USA): Computers and Structures INC; 2006.

[7]. A. Kadid and A. Boumrkik, “Pushover analysis of reinforced concrete frame structures”, Asian journal of civil engineering (building and housing) Vol. 9, No.1, pp. 75-83, 2008.

[8]. A. Ghaffar, A. Javed, H. Rehman, K. Ahmed and Mhyas, “Development of shear capacity equations for rectangular reinforced beams”, Park J Eng. & appl.Sci.Vol.6, pp.

[9]. Alexander Placas and Paul E. Regan and A.L.L Baker, “Shear failure of reinforced concrete beams," ACI journal, title No.68-67, pp.763-773, October 1971.

[10]. G. Russo, G. Somma and P. Angeli, “Design Shear Strength Formula for High Strength Concrete Beams”, Journal of Material and Structures, 10(37), pp. 1519–1527, 2004.

[11]. G. A. Rao and S. S. Injaganeri, “Evaluation of size dependent design shear strength of reinforced concrete beams without web reinforcement”, Sadhana Vol.36, Part 3, pp.393-410, 2011.

[12]. Gastebled, Olivier J. and May Lan M, “Fracture Mechanics Model Applied to Shear Failure of Reinforced Concrete Beams without Stirrups”, ACI Structural Journal, pp.184-190, 1998.

[13]. Gerin, M. and Adebar P., “Accounting for shear in seismic analysis of concrete structures”, in Proceedings of the 13th World Conference on Earthquake Engineering, paper 1747. Vancouver, B.C., Canada, Aug. 2004.

[14]. H.Sezen and E.J.Setzle, “Model for the lateral behaviour of reinforced concrete columns including shear deformations earthquake spectra”, Vol. 24, No. 2, pages 493–511, May 2008.

[15]. IITM-SERC Manual, “Manual on seismic evaluations and retrofitting of RC building multi-storied RC building”, March 2005.

[16]. ACI 318, “Building Code Requirements for Reinforced Concrete, American Concrete Institute”, Detroit, Michigan, 2002.

[17]. SAP 2000 (Version 11.0), Integrated Software for Structural Analysis and Design. Computers & Structures, Inc., Berkeley, California, 2007.

[18]. Kani G N J, “The basic facts concerning shear failure”, Proc. ACI Journal., 63(7), pp. 675–692, 1966.